Hadronic charmless B decays $B \to AP$

Hai-Yang Cheng[1] and Kwei-Chou Yang[2]

[1]*Institute of Physics, Academia Sinica, Taipei, Taiwan 115, Republic of China*

[2]*Department of Physics, Chung Yuan Christian University, Chung-Li, Taiwan 320, Republic of China*

(Received 4 September 2007; published 28 December 2007)

The two-body hadronic decays of B mesons into pseudoscalar and axial-vector mesons are studied within the framework of QCD factorization. The light cone distribution amplitudes (LCDAs) for $^3P_1$ and $^1P_1$ axial-vector mesons have been evaluated using the QCD sum rule method. Owing to the G-parity, the chiral-even two-parton light cone distribution amplitudes of the $^3P_1$ ($^1P_1$) mesons are symmetric (antisymmetric) under the exchange of quark and antiquark momentum fractions in the SU(3) limit. For chiral-odd LCDAs, it is the other way around. The main results are the following: (i) The predicted rates for $a_1^\pm(1260)\pi^\mp$, $b_1^\pm(1235)\pi^\mp$, $b_1^0(1235)\pi^-$, $a_1^+K^-$, and $b_1^+K^-$ modes are in good agreement with the data. However, the naively expected ratios $\mathcal{B}(B^- \to a_1^0\pi^-)/\mathcal{B}(\bar{B}^0 \to a_1^+\pi^-) \lesssim 1$, $\mathcal{B}(B^- \to a_1^-\pi^0)/\mathcal{B}(\bar{B}^0 \to a_1^-\pi^+) \sim \frac{1}{2}$, and $\mathcal{B}(B^- \to b_1^0K^-)/\mathcal{B}(\bar{B}^0 \to b_1^+K^-) \sim \frac{1}{2}$ are not borne out by experiment. This should be clarified by the improved measurements of these decays. (ii) Since the $\bar{B} \to b_1K$ decays receive sizable annihilation contributions, their rates are sensitive to the interference between penguin and annihilation terms. The measurement of $\mathcal{B}(\bar{B}^0 \to b_1^+K^-)$ implies a destructive interference which in turn indicates that the form factors for $B \to b_1$ and $B \to a_1$ transitions are of opposite signs. (iii) Sizable power corrections such as weak annihilation are needed to account for the observed rates of the penguin-dominated modes $K_1^-(1270)\pi^+$ and $K_1^-(1400)\pi^+$. (iv) The decays $B \to K_1\bar{K}$ with $K_1 = K_1(1270)$, $K_1(1400)$ are in general quite suppressed, of order 10^{-7}–10^{-8}, except for $\bar{B}^0 \to \bar{K}_1^0(1270)K^0$ which can have a branching ratio of order 2.3×10^{-6}. The decay modes $K_1^-K^+$ and $K_1^+K^-$ are of particular interest as they proceed only through weak annihilation. (v) The mixing-induced parameter S is predicted to be negative in the decays $B^0 \to a_1^\pm\pi^\mp$, while it is positive experimentally. This may call for a larger unitarity angle $\gamma \gtrsim 80°$. (vi) Branching ratios for the decays $B \to f_1\pi$, f_1K, $h_1\pi$ and h_1K with $f_1 = f_1(1285)$, $f_1(1420)$ and $h_1 = h_1(1170)$, $h_1(1380)$ are generally of order 10^{-6} except for the color-suppressed modes $f_1\pi^0$ and $h_1\pi^0$ which are suppressed by 1 to 2 orders of magnitude. Measurements of the ratios $\mathcal{B}(B^- \to h_1(1380)\pi^-)/\mathcal{B}(B^- \to h_1(1170)\pi^-)$ and $\mathcal{B}(\bar{B} \to f_1(1420)\bar{K})/\mathcal{B}(\bar{B} \to f_1(1285)\bar{K})$ will help determine the mixing angles $\theta_{^1P_1}$ and $\theta_{^3P_1}$, respectively.

DOI: 10.1103/PhysRevD.76.114020 PACS numbers: 13.25.Hw, 12.38.Bx, 14.40.−n

I. INTRODUCTION

In the quark model, two nonets of $J^P = 1^+$ axial-vector mesons are expected as the orbital excitation of the $q\bar{q}$ system. In terms of the spectroscopic notation $^{2S+1}L_J$, there are two types of p-wave mesons, namely, $^3P_1$ and $^1P_1$. These two nonets have distinctive C quantum numbers, $C = +$ and $C = -$, respectively. Experimentally, the $J^{PC} = 1^{++}$ nonet consists of $a_1(1260)$, $f_1(1285)$, $f_1(1420)$, and K_{1A}, while the 1^{+-} nonet has $b_1(1235)$, $h_1(1170)$, $h_1(1380)$, and K_{1B}. The physical mass eigenstates $K_1(1270)$ and $K_1(1400)$ are a mixture of K_{1A} and K_{1B} states owing to the mass difference of the strange and nonstrange light quarks.

The production of the axial-vector mesons has been seen in the two-body hadronic D decays: $D \to Ka_1(1260)$, $D^0 \to K_1^-(1270)\pi$ and $D^+ \to K_1^0(1400)\pi$, and in charmful B decays: $B \to J/\psi K_1(1270)$ and $B \to Da_1(1260)$ [1]. As for charmless hadronic B decays, $B^0 \to a_1^\pm(1260)\pi^\mp$ are the first modes measured by both B factories, *BABAR* and Belle. The *BABAR* result is [2]

$$\mathcal{B}(B^0 \to a_1^\pm(1260)\pi^\mp) = (33.2 \pm 3.8 \pm 3.0) \times 10^{-6}, \tag{1.1}$$

where the assumption of $\mathcal{B}(a_1^\pm \to \pi^\pm\pi^\pm\pi^\mp) = 1/2$ has been made. The Belle measurement gives [3]

$$\mathcal{B}(B^0 \to a_1^\pm(1260)\pi^\mp) = (29.8 \pm 3.2 \pm 4.6) \times 10^{-6}. \tag{1.2}$$

The average of the two experiments is

$$\mathcal{B}(B^0 \to a_1^\pm(1260)\pi^\mp) = (31.7 \pm 3.7) \times 10^{-6}. \tag{1.3}$$

Moreover, *BABAR* has also measured the time-dependent CP asymmetries in $B^0 \to a_1^\pm(1260)\pi^\mp$ decays [4]. From the measured CP parameters, one can determine the decay rates of $a_1^+\pi^-$ and $a_1^-\pi^+$ separately [4]. Recently, *BABAR* has reported the observation of the decays $\bar{B}^0 \to b_1^\pm\pi^\mp$, $b_1^+K^-$ and $B^- \to b_1^0\pi^-$, $b_1^0K^-$, $a_1^0\pi^-$, $a_1^-\pi^0$ [5,6]. The preliminary *BABAR* results for $\bar{B}^0 \to K_1^-(1270)\pi^+$, $K_1^-(1400)\pi^+$, $a_1^+K^-$, $B^- \to a_1^-\bar{K}^0$, $f_1(1285)K^-$, $f_1(1420)K^-$ are also available recently [7–10].

In the present work we will focus on the B decays involving an axial-vector meson A and a pseudoscalar meson P in the final state. Since the $^3P_1$ meson behaves similarly to the vector meson, it is naively expected that AP

modes have similar rates as VP ones, for example, $\mathcal{B}(B^0 \to a_1^{\pm}(1260)\pi^{\mp}) \sim \mathcal{B}(B^0 \to \rho^{\pm}\pi^{\mp})$. However, this will not be the case for the $^1P_1$ meson. First of all, its decay constant vanishes in the SU(3) limit. For example, the decay constant vanishes for the neutral $b_1^0(1235)$ and is very small for the charged $b_1(1235)$ states. This feature can be checked experimentally by measuring $B^0 \to b_1^+\pi^-$, $b_1^-\pi^+$ decays and seeing if the former is suppressed relative to the latter. Second, its chiral-even two-parton light cone distribution amplitude (LCDA) is antisymmetric under the exchange of quark and antiquark momentum fractions in the SU(3) limit due to the G parity, contrary to the symmetric behavior for the $^3P_1$ meson.

Charmless $B \to AP$ and $B \to AV$ decays have been studied in the literature [11–16]. Except for [11,16], most of the existing calculations were carried out in the framework of either naive factorization or generalized factorization in which the nonfactorizable effects are described by the parameter $N_c^{\rm eff}$, the effective number of colors. In the approach of QCD factorization, nonfactorizable effects such as vertex corrections, hard spectator interactions and annihilation contributions are calculable and have been considered in [11,16] for the decays $B \to a_1(1260)\pi$, $a_1(1260)K$, $B \to h_1(1235)K^*$, $b_1(1235)K^*$, and $b_1(1235)\rho$.

One crucial ingredient in QCDF calculations is the LCDAs for $^3P_1$ and $^1P_1$ axial-vector mesons. In general, the LCDAs are expressed in terms of the expansion of Gegenbauer moments which have been systematically studied by one of us (K.C.Y.) using the light cone sum rule method [17,18]. Armed with the LCDAs, one is able to explore the nonfactorizable corrections to the naive factorization.

The present paper is organized as follows. In Sec. II we summarize all the input parameters relevant to the present work, such as the mixing angles, decay constants, form factors, and light cone distribution amplitudes for $^3P_1$ and $^1P_1$ axial-vector mesons. We then apply QCD factorization in Sec. III to study $B \to AP$ decays. Results and discussions are presented in Sec. IV. Sec. V contains our conclusions. The factorizable amplitudes of various $B \to AV$ decays are summarized in the appendix.

II. INPUT PARAMETERS

A. Mixing angles

In the quark model, there are two different types of light axial-vector mesons: $^3P_1$ and $^1P_1$, which carry the quantum numbers $J^{\rm PC} = 1^{++}$ and 1^{+-}, respectively. The 1^{++} nonet consists of $a_1(1260)$, $f_1(1285)$, $f_1(1420)$, and K_{1A}, while the 1^{+-} nonet has $b_1(1235)$, $h_1(1170)$, $h_1(1380)$, and K_{1B}. The nonstrange axial-vector mesons, for example, the neutral $a_1(1260)$ and $b_1(1235)$ cannot have mixing because of the opposite C-parities. On the contrary, the strange partners of $a_1(1260)$ and $b_1(1235)$, namely, K_{1A} and K_{1B}, respectively, are not mass eigenstates and they are mixed together due to the strange and nonstrange light quark mass difference. We write

$$\begin{aligned} K_1(1270) &= K_{1A}\sin\theta_{K_1} + K_{1B}\cos\theta_{K_1}, \\ K_1(1400) &= K_{1A}\cos\theta_{K_1} - K_{1B}\sin\theta_{K_1}. \end{aligned} \tag{2.1}$$

If the mixing angle is 45° and $\langle K\rho|K_{1B}\rangle = \langle K\rho|K_{1A}\rangle$, one can show that $K_1(1270)$ is allowed to decay into $K\rho$ but not $K^*\pi$, and vice versa for $K_1(1400)$ [19].

From the experimental information on masses and the partial rates of $K_1(1270)$ and $K_1(1400)$, Suzuki found two possible solutions with a twofold ambiguity, $|\theta_{K_1}| \approx 33^\circ$ and 57° [20]. A similar constraint $35^\circ \lesssim |\theta_{K_1}| \lesssim 55^\circ$ is obtained in [21] based solely on two parameters: the mass difference of the a_1 and b_1 mesons and the ratio of the constituent quark masses. From the data of $\tau \to K_1(1270)\nu_\tau$ and $K_1(1400)\nu_\tau$ decays, the mixing angle is extracted to be $\pm 37^\circ$ and $\pm 58^\circ$ in [22]. As for the sign of the mixing angle, there is an argument favoring a negative θ_{K_1}. It has been pointed out in [23] that the experimental measurement of the ratio of $K_1\gamma$ production in B decays can be used to fix the sign of the mixing angle. Based on the covariant light-front quark model [24], it is found [23][1]

$$\frac{\mathcal{B}(B \to K_1(1270)\gamma)}{\mathcal{B}(B \to K_1(1400)\gamma)} = \begin{cases} 10.1 \pm 6.2\ (280 \pm 200); & \text{for } \theta_{K_1} = -58^\circ(-37^\circ), \\ 0.02 \pm 0.02\ (0.05 \pm 0.04); & \text{for } \theta_{K_1} = +58^\circ(+37^\circ). \end{cases} \tag{2.2}$$

The Belle measurements $\mathcal{B}(B^+ \to K_1^+(1270)\gamma) = (4.3 \pm 0.9 \pm 0.9) \times 10^{-5}$ and $\mathcal{B}(B^+ \to K_1^+(1400)\gamma) < 1.5 \times 10^{-5}$ [25] clearly favor $\theta_{K_1} = -58^\circ$ over $\theta_{K_1} = 58^\circ$ and $\theta_{K_1} = -37^\circ$ over $\theta_{K_1} = 37^\circ$. In the ensuing discussions we will fix the sign of θ_{K_1} to be negative.

[1]The sign of θ_{K_1} is intimately related to the relative sign of the K_{1A} and K_{1B} states. In the light-front quark model used in [23,24], the decay constants of K_{1A} and K_{1B} are of opposite sign, while the $B \to K_{1A}$ and $B \to K_{1B}$ form factors are of the same sign. It is the other way around in the present work: the decay constants of K_{1A} and K_{1B} have the same signs, while the $B \to K_{1A}$ and $B \to K_{1B}$ form factors are opposite in sign. The two schemes are related via a redefinition of the K_{1A} or K_{1B} state, i.e. $K_{1A} \to -K_{1A}$ or $K_{1B} \to -K_{1B}$. To write down Eq. (2.2) we have used our convention for K_{1A} and K_{1B} states.

Likewise, the ${}^3P_1$ states $f_1(1285)$ and $f_1(1420)$ have mixing due to SU(3) breaking effects

$$\begin{aligned} |f_1(1285)\rangle &= |f_1\rangle \cos\theta_{{}^3P_1} + |f_8\rangle \sin\theta_{{}^3P_1}, \\ |f_1(1420)\rangle &= -|f_1\rangle \sin\theta_{{}^3P_1} + |f_8\rangle \cos\theta_{{}^3P_1}. \end{aligned} \tag{2.3}$$

From the Gell-Mann-Okubo mass formula [1,26], it follows that

$$\cos^2\theta_{{}^3P_1} = \frac{4m_{K_{1A}}^2 - m_{a_1}^2 - 3m_{f_1(1285)}^2}{3(m_{f_1(1420)}^2 - m_{f_1(1285)}^2)}, \tag{2.4}$$

where

$$m_{K_{1A}}^2 = m_{K_1(1400)}^2 \cos^2\theta_{K_1} + m_{K_1(1270)}^2 \sin^2\theta_{K_1}. \tag{2.5}$$

Substituting this into Eq. (2.4) with $\theta_{K_1} = -37^\circ(-58^\circ)$, we then obtain $\theta_{{}^3P_1}^{\rm quad} = 27.9^\circ(53.2^\circ)$ and $\theta_{{}^3P_1}^{\rm lin} = 26.0^\circ(52.1)^\circ$ where the latter is obtained by replacing the meson mass squared m^2 by m throughout Eq. (2.4). The sign of the mixing angle can be determined from the mass relation [1]

$$\tan\theta_{{}^3P_1} = \frac{4m_{K_{1A}}^2 - m_{a_1}^2 - 3m_{f_1(1420)}^2}{2\sqrt{2}(m_{a_1}^2 - m_{K_{1A}}^2)}. \tag{2.6}$$

The previous phenomenological analyses suggest that $\theta_{{}^3P_1} \simeq 50^\circ$ [27].[2] Eliminating θ from Eqs. (2.4) and (2.6) leads to the sum rule

$$\begin{aligned} &(m_{f_1(1285)}^2 + m_{f_1(1400)}^2)(4m_{K_{1A}}^2 - m_{a_1}^2) - 3m_{f_1(1285)}^2 m_{f_1(1400)}^2 \\ &= 8m_{K_{1A}}^4 - 8m_{K_{1A}}^2 m_{a_1}^2 + 3m_{a_1}^4. \end{aligned} \tag{2.7}$$

This relation is satisfied for ${}^3P_1$ octet mesons, but only approximately for ${}^1P_1$ states. Anyway, we shall use the mass relation (2.4) to fix the magnitude of the mixing angle and (2.6) to fix its sign.

Since $K^*\bar{K}$ and $K\bar{K}\pi$ are the dominant modes of $f_1(1420)$ whereas $f_0(1285)$ decays mainly to the 4π states, this suggests that the quark content is primarily $s\bar{s}$ for $f_1(1420)$ and $n\bar{n}$ for $f_1(1285)$. This may indicate that $\theta_{{}^3P_1} = 28^\circ$ is slightly preferred. However, $\theta_{{}^3P_1} = 53^\circ$ is equally acceptable.

Similarly, for $1{}^1P_1$ states, $h_1(1170)$ and $h_1(1380)$ may be mixed in terms of the pure octet h_8 and singlet h_1,

$$\begin{aligned} |h_1(1170)\rangle &= |h_1\rangle \cos\theta_{{}^1P_1} + |h_8\rangle \sin\theta_{{}^1P_1}, \\ |h_1(1380)\rangle &= -|h_1\rangle \sin\theta_{{}^1P_1} + |h_8\rangle \cos\theta_{{}^1P_1}. \end{aligned} \tag{2.8}$$

Again from the Gell-Mann-Okubo mass formula, we obtain

$$\cos^2\theta_{{}^1P_1} = \frac{4m_{K_{1B}}^2 - m_{b_1}^2 - 3m_{h_1(1170)}^2}{3(m_{h_1(1380)}^2 - m_{h_1(1170)}^2)}, \tag{2.9}$$

where

$$m_{K_{1B}}^2 = m_{K_1(1400)}^2 \sin^2\theta_{K_1} + m_{K_1(1270)}^2 \cos^2\theta_{K_1}. \tag{2.10}$$

We obtain $\theta_{{}^1P_1}^{\rm quad} = -18.1^\circ(25.2^\circ)$ and $\theta_{{}^1P_1}^{\rm lin} = 23.8^\circ(-18.3^\circ)$ for $\theta_{K_1} = -37^\circ(-58^\circ)$, where the sign of the mixing angle is determined from the mass relation

$$\tan\theta_{{}^1P_1} = \frac{4m_{K_{1B}}^2 - m_{b_1}^2 - 3m_{h_1(1170)}^2}{2\sqrt{2}(m_{b_1}^2 - m_{K_{1B}}^2)}. \tag{2.11}$$

B. Decay constants

Decay constants of pseudoscalar and axial-vector mesons are defined as

$$\begin{aligned} \langle P(p)|\bar{q}_2\gamma_\mu\gamma_5 q_1|0\rangle &= -if_P q_\mu, \\ \langle {}^{3(1)}P_1(p,\lambda)|\bar{q}_2\gamma_\mu\gamma_5 q_1|0\rangle &= if_{{}^3P_1({}^1P_1)} m_{{}^3P_1({}^1P_1)} \epsilon_\mu^{(\lambda)*}. \end{aligned} \tag{2.12}$$

For axial-vector mesons, the transverse decay constant is defined via the tensor current by

$$\langle {}^{3(1)}P_1(p,\lambda)|\bar{q}_2\sigma^{\mu\nu}\gamma_5 q_1|0\rangle = -f_{{}^{3(1)}P_1}^\perp (\epsilon_{(\lambda)}^{*\mu} p^\nu - \epsilon_{(\lambda)}^{*\nu} p^\mu), \tag{2.13}$$

or

$$\langle {}^{3(1)}P_1(p,\lambda)|\bar{q}_2\sigma^{\mu\nu} q_1|0\rangle = -if_{{}^{3(1)}P_1}^\perp \epsilon_{\mu\nu\alpha\beta}\epsilon_{(\lambda)}^{*\alpha} p^\beta, \tag{2.14}$$

where we have applied the identity $\sigma_{\alpha\beta}\gamma_5 = -\frac{i}{2}\epsilon_{\alpha\beta\mu\nu}\sigma^{\mu\nu}$ with the sign convention $\epsilon_{0123} = 1$. Since the tensor current is not conserved, the transverse decay constant $f^\perp$ is scale dependent. Because of charge conjugation invariance, the decay constant of the ${}^1P_1$ nonstrange neutral meson $b_1^0(1235)$ must be zero. In the isospin limit, the decay constant of the charged b_1 vanishes due to the fact that the b_1 has even G-parity and that the relevant weak axial-vector current is odd under G transformation. Hence, $f_{b_1^\pm}$ is very small in reality. Note that the matrix element of the pseudoscalar density vanishes, $\langle {}^{3(1)}P_1(p,\varepsilon)|\bar{q}_2\gamma_5 q_1|0\rangle = 0$, which can be seen by applying the equation of motion. As for the strange axial-vector mesons, the ${}^3P_1$ and ${}^1P_1$ states transfer under charge conjugation as

$$M_a^b({}^3P_1) \to M_b^a({}^3P_1), \qquad M_a^b({}^1P_1) \to -M_b^a({}^1P_1), \qquad (a,b = 1,2,3). \tag{2.15}$$

Since the weak axial-vector current transfers as $(A_\mu)_a^b \to (A_\mu)_b^a$ under charge conjugation, it is clear that $f_{{}^1P_1} = 0$ in the SU(3) limit [20]. By the same token, the decay constant

[2] If a mixing angle $\theta_{{}^3P_1}$ of order 50° can be independently inferred from other processes, this will imply a preference of $|\theta_{K_1}| = 58^\circ$ over $|\theta_{K_1}| = 37^\circ$. However, the phenomenological analysis in [27] is not robust and the Gell-Mann-Okubo mass formula employed there is not a correct one.

$f^{\perp}_{^3P_1}$ vanishes in the SU(3) limit. Note for scalar mesons, their decay constants also vanish in the same limit, which can be easily seen by applying equations of motion to obtain

$$m_S^2 f_S = i(m_1 - m_2)\langle 0|\bar{q}_1 q_2|S\rangle, \tag{2.16}$$

with m_i being the mass of the quark q_i.

The $a_1(1260)$ decay constant $f_{a_1} = 238 \pm 10$ MeV obtained using the QCD sum rule method [18] is similar to the ρ meson one, $f_\rho \approx 216$ MeV. This means that the $a_1(1260)$ can be regarded as the scalar partner of the ρ, as it should be. To compute the decay constant f_{b_1} for the charged b_1, one needs to specify the u and d quark mass difference in the model calculation. In the covariant light-front quark model [24], if we increase the constituent d quark mass by an amount of 5 ± 2 MeV relative to the u quark one, we find $f_{b_1} = 0.6 \pm 0.2$ MeV which is highly suppressed. As we shall see below, the decay constant f_{b_1} is related to the transverse one $f^{\perp}_{b_1}$ by the relation [see Eq. (2.65)]

$$f_{b_1} = f^{\perp}_{b_1}(\mu) a_0^{\parallel, b_1}(\mu), \tag{2.17}$$

where $a_0^{\parallel,b_1}$ is the zeroth Gegenbauer moment of $\Phi_\parallel^{b_1}$ to be defined later. The quantities $f^{\perp}_{b_1}$ and $a_0^{\parallel,b_1}$ can be calculated in the QCD sum rule approach with the results $f^{\perp}_{b_1} = (180 \pm 8)$ MeV [18] (cf. Table I) and $a_0^{\parallel,b_1} = 0.0028 \pm 0.0026$ for b_1^- at $\mu = 1$ GeV. (Note that for b_1^+, $a_0^{\parallel,b_1}$ has an opposite sign due to G-parity.) Again, f_{b_1} is very small, of order 0.5 MeV, in agreement with the estimation based on the light-front quark model. In [14], the decay constants of a_1 and b_1 are derived using the $K_{1A} - K_{1B}$ mixing angle θ_{K_1} and SU(3) symmetry: $(f_{b_1}, f_{a_1}) = (74, 215)$ MeV for $\theta_{K_1} = 32^\circ$ and $(-28\,223)$ MeV for $\theta_{K_1} = 58^\circ$. It seems to us that the b_1 decay constant derived in this manner is too big.

Introducing the decay constants $f^q_{f_1(1285)}$ and $f^q_{f_1(1420)}$ by

$$\langle 0|\bar{q}\gamma_\mu\gamma_5 q|f_1(1285)(P,\lambda)\rangle = -im_{f_1(1285)} f^q_{f_1(1285)} \epsilon_\mu^{(\lambda)}, \tag{2.18}$$

TABLE I. Summary of the decay constants $f_{^3P_1}$ and $f^{\perp}_{^1P_1}(1\text{ GeV})$ in units of MeV obtained from QCD sum rule methods [18].

$^3P_1$	$a_1(1260)$	f_1	f_8	K_{1A}
$f_{^3P_1}$	238 ± 10	245 ± 13	239 ± 13	250 ± 13
$^1P_1$	$b_1(1235)$	h_1	h_8	K_{1B}
$f^{\perp}_{^1P_1}$	180 ± 8	180 ± 12	190 ± 10	190 ± 10

$$\langle 0|\bar{q}\gamma_\mu\gamma_5 q|f_1(1420)(P,\lambda)\rangle = -im_{f_1(1420)} f^q_{f_1(1420)} \epsilon_\mu^{(\lambda)}, \tag{2.19}$$

we obtain

$$\begin{aligned} f^u_{f_1(1285)} &= \frac{f_{f_1}}{\sqrt{3}} \frac{m_{f_1}}{m_{f_1(1285)}} \cos\theta_{^3P_1} + \frac{f_{f_8}}{\sqrt{6}} \frac{m_{f_8}}{m_{f_1(1285)}} \sin\theta_{^3P_1} \\ &= 172 \pm 23\ (178 \pm 22)\ \text{MeV}, \end{aligned} \tag{2.20}$$

$$\begin{aligned} f^s_{f_1(1285)} &= \frac{f_{f_1}}{\sqrt{3}} \frac{m_{f_1}}{m_{f_1(1285)}} \cos\theta_{^3P_1} - \frac{2f_{f_8}}{\sqrt{6}} \frac{m_{f_8}}{m_{f_1(1285)}} \sin\theta_{^3P_1} \\ &= -72 \pm 13\ (29 \pm 18)\ \text{MeV}, \end{aligned} \tag{2.21}$$

$$\begin{aligned} f^u_{f_1(1420)} &= -\frac{f_{f_1}}{\sqrt{3}} \frac{m_{f_1}}{m_{f_1(1420)}} \sin\theta_{^3P_1} + \frac{f_{f_8}}{\sqrt{6}} \frac{m_{f_8}}{m_{f_1(1420)}} \cos\theta_{^3P_1} \\ &= -55 \pm 10\ (23 \pm 11)\ \text{MeV}, \end{aligned} \tag{2.22}$$

$$\begin{aligned} f^s_{f_1(1420)} &= -\frac{f_{f_1}}{\sqrt{3}} \frac{m_{f_1}}{m_{f_1(1420)}} \sin\theta_{^3P_1} - \frac{2f_{f_8}}{\sqrt{6}} \frac{m_{f_8}}{m_{f_1(1420)}} \cos\theta_{^3P_1} \\ &= -219 \pm 27\ (-230 \pm 26)\ \text{MeV}, \end{aligned} \tag{2.23}$$

corresponding to $\theta_{^3P_1} = 53.2^\circ(27.9^\circ)$, where we have used the QCD sum rule results for f_{f_1} and f_{f_8} [18] (see Table I).

The decay constants for $K_1(1270)$ and $K_1(1400)$ defined by (with $\bar{q} = \bar{u}$ or $\bar{d}$)

$$\langle 0|\bar{q}\gamma_\mu\gamma_5 s|K_1(1270)(P,\lambda)\rangle = -if_{K_1(1270)} m_{K_1(1270)} \epsilon_\mu^{(\lambda)}, \tag{2.24}$$

and

$$\langle 0|\bar{q}\gamma_\mu\gamma_5 s|K_1(1400)(P,\lambda)\rangle = -if_{K_1(1400)} m_{K_1(1400)} \epsilon_\mu^{(\lambda)} \tag{2.25}$$

are related to $f_{K_{1A}}$ and $f_{K_{1B}}$ by

$$\begin{aligned} f_{K_1(1270)} &= \frac{1}{m_{K_1(1270)}}(f_{K_{1A}} m_{K_{1A}} \sin\theta_{K_1} + f_{K_{1B}} m_{K_{1B}} \cos\theta_{K_1}), \\ f_{K_1(1400)} &= \frac{1}{m_{K_1(1400)}}(f_{K_{1A}} m_{K_{1A}} \cos\theta_{K_1} - f_{K_{1B}} m_{K_{1B}} \sin\theta_{K_1}). \end{aligned} \tag{2.26}$$

Just as the previous b_1 case, the decay constant $f_{K_{1B}}$ is related to the transverse one $f^{\perp}_{K_{1B}}$ by the relation $f_{K_{1B}} = f^{\perp}_{K_{1B}}(\mu) a_0^{\parallel,K_{1B}}(\mu)$. If we apply the QCD sum rule results for $f_{K_{1A}}$, $f^{\perp}_{K_{1B}}$ (see Table I) and $a_0^{\parallel,K_{1B}}$ (cf. Table V), we will obtain

$$\begin{aligned} f_{K_1(1270)} &= -137 \pm 15 \text{ MeV}, \\ f_{K_1(1400)} &= 199 \pm 10 \text{ MeV}, \quad \text{for } \theta_{K_1} = -37^\circ, \\ f_{K_1(1270)} &= -207 \pm 7 \text{ MeV}, \\ f_{K_1(1400)} &= 141 \pm 14 \text{ MeV}, \quad \text{for } \theta_{K_1} = -58^\circ. \end{aligned} \tag{2.27}$$

However, we would like to make two remarks. First, we do have the experimental information on the decay constant of $K_1(1270)$.[3] From the measured branching ratio of $\tau \to K_1^-(1270)\nu_\tau$ by ALEPH [28], $\mathcal{B}(\tau^- \to K_1^-(1270)\nu_\tau) = (4.7 \pm 1.1) \times 10^{-3}$, the decay constant of $K_1(1270)$ is extracted to be [22]

$$|f_{K_1(1270)}| = 175 \pm 19 \text{ MeV}, \tag{2.28}$$

where use has been made of the formula

$$\Gamma(\tau \to K_1 \nu_\tau) = \frac{G_F^2}{16\pi} |V_{us}|^2 f_{K_1}^2 \frac{(m_\tau^2 + 2m_{K_1}^2)(m_\tau^2 - m_{K_1}^2)^2}{m_\tau^3}. \tag{2.29}$$

Second, as pointed out in [24], the decay constants of $^3P_1$ have opposite signs to that of $^1P_1$ in the covariant light-front quark model. The large error with the QCD sum rule result of $a_0^{\parallel, K_{1B}} = 0.14 \pm 0.15$ is already an indication of possible large sum rule uncertainties in this quantity.

In order to reduce the theoretical uncertainties with the K_1 decay constant, we shall use the experimental value of $f_{K_1(1270)}$ to fix the input parameters $\beta_{K_{1A}}$ and $\beta_{K_{1B}}$ appearing in the Gaussian-type wave function in the covariant quark model [24]. We obtain

$$\beta_{K_{1A}} = \beta_{K_{1B}} = \begin{cases} 0.375 \text{ GeV}; & \text{for } \theta_{K_1} = -37^\circ, \\ 0.313 \text{ GeV}; & \text{for } \theta_{K_1} = -58^\circ, \end{cases} \tag{2.30}$$

and

$$\begin{aligned} f_{K_{1A}} &= 293 \text{ MeV}, \\ f_{K_{1B}} &= 15 \text{ MeV}, \quad \text{for } \theta_{K_1} = -37^\circ, \\ f_{K_{1A}} &= 207 \text{ MeV}, \\ f_{K_{1B}} &= 12 \text{ MeV}, \quad \text{for } \theta_{K_1} = -58^\circ. \end{aligned} \tag{2.31}$$

Therefore, we have

$$\begin{aligned} f_{K_1(1270)} &= -175 \pm 11 \text{ MeV}, \\ f_{K_1(1400)} &= 235 \pm 12 \text{ MeV}, \quad \text{for } \theta_{K_1} = -37^\circ, \\ f_{K_1(1270)} &= -175 \pm 15 \text{ MeV}, \\ f_{K_1(1400)} &= 112 \pm 12 \text{ MeV}, \quad \text{for } \theta_{K_1} = -58^\circ. \end{aligned} \tag{2.32}$$

In complete analogy to the discussion for 1^3P_1 states, we introduce the tensor couplings for 1^1P_1 states

$$\langle 0|\bar{q}\sigma_{\mu\nu}q|h_1(1170)(P,\lambda)\rangle = i f^{\perp,q}_{h_1(1170)} \epsilon_{\mu\nu\alpha\beta}\epsilon^\alpha_{(\lambda)} P^\beta, \tag{2.33}$$

$$\langle 0|\bar{q}\sigma_{\mu\nu}q|h_1(1380)(P,\lambda)\rangle = i f^{\perp,q}_{h_1(1380)} \epsilon_{\mu\nu\alpha\beta}\epsilon^\alpha_{(\lambda)} P^\beta, \tag{2.34}$$

and then obtain

$$\begin{aligned} f^{\perp,u}_{h_1(1170)} &= \frac{f^\perp_{h_1}}{\sqrt{3}} \cos\theta_{^1P_1} + \frac{f^\perp_{h_8}}{\sqrt{6}} \sin\theta_{^1P_1} \\ &= 75 \pm 8 \ (127 \pm 7) \text{ MeV}, \end{aligned} \tag{2.35}$$

$$\begin{aligned} f^{\perp,s}_{h_1(1170)} &= \frac{f^\perp_{h_1}}{\sqrt{3}} \cos\theta_{^1P_1} - \frac{2f^\perp_{h_8}}{\sqrt{6}} \sin\theta_{^1P_1} \\ &= 147 \pm 8 \ (28 \pm 10) \text{ MeV}, \end{aligned} \tag{2.36}$$

$$\begin{aligned} f^{\perp,u}_{h_1(1380)} &= -\frac{f^\perp_{h_1}}{\sqrt{3}} \sin\theta_{^1P_1} + \frac{f^\perp_{h_8}}{\sqrt{6}} \cos\theta_{^1P_1} \\ &= 106 \pm 5 \ (26 \pm 7) \text{ MeV}, \end{aligned} \tag{2.37}$$

$$\begin{aligned} f^{\perp,s}_{h_1(1380)} &= -\frac{f^\perp_{h_1}}{\sqrt{3}} \sin\theta_{^1P_1} - \frac{2f^\perp_{h_8}}{\sqrt{6}} \cos\theta_{^1P_1} \\ &= -115 \pm 9 \ (-185 \pm 10) \text{ MeV}, \end{aligned} \tag{2.38}$$

corresponding to $\theta_{^1P_1} = -18.1^\circ(25.2^\circ)$ where we have used the QCD sum rule results for $f^\perp_{h_1}$ and $f^\perp_{h_8}$ given in Table I [18].

As for strange axial-vector mesons, we have (with $\bar{q} \equiv \bar{u}, \bar{d}$)

$$\langle 0|\bar{q}\sigma_{\mu\nu}s|K_1(1270)(p,\lambda)\rangle = i f^\perp_{K_1(1270)} \epsilon_{\mu\nu\alpha\beta}\epsilon^\alpha_{(\lambda)} p^\beta = i(f^\perp_{K_{1A}} \sin\theta_{K_1} + f^\perp_{K_{1B}} \cos\theta_{K_1})\epsilon_{\mu\nu\alpha\beta}\epsilon^\alpha_{(\lambda)} p^\beta \tag{2.39}$$

and

$$\langle 0|\bar{q}\sigma_{\mu\nu}s|K_1(1400)(p,\lambda)\rangle = i f^\perp_{K_1(1400)} \epsilon_{\mu\nu\alpha\beta}\epsilon^\alpha_{(\lambda)} p^\beta = i(f^\perp_{K_{1A}} \cos\theta_{K_1} - f^\perp_{K_{1B}} \sin\theta_{K_1})\epsilon_{\mu\nu\alpha\beta}\epsilon^\alpha_{(\lambda)} p^\beta. \tag{2.40}$$

[3]The large experimental error with the $K_1(1400)$ production in the τ decay, namely, $\mathcal{B}(\tau^- \to K_1^-(1400)\nu_\tau) = (1.7 \pm 2.6) \times 10^{-3}$ [1], does not provide sensible information for the $K_1(1400)$ decay constant.

As will be shown in Sec. II D below, the decay constants $f_{K_{1A}}$ and $f^{\perp}_{K_{1A}}$ are related via

$$f^{\perp}_{K_{1A}}(\mu) = f_{K_{1A}} a_0^{\perp,K_{1A}}(\mu). \tag{2.41}$$

From Tables I and V, we obtain (at the scale $\mu = 1$ GeV)

$$\begin{aligned} f^{\perp}_{K_1(1270)} &= 140 \pm 22 \text{ MeV}, \\ f^{\perp}_{K_1(1400)} &= 130 \pm 25 \text{ MeV}, \quad \text{for } \theta_{K_1} = -37^\circ, \\ f^{\perp}_{K_1(1270)} &= 84 \pm 25 \text{ MeV}, \\ f^{\perp}_{K_1(1400)} &= 172 \pm 21 \text{ MeV}, \quad \text{for } \theta_{K_1} = -58^\circ. \end{aligned} \tag{2.42}$$

C. Form factors

The form factors for the $\bar{B} \to A$ and $\bar{B} \to P$ transitions are defined as

$$\begin{aligned} \langle A(p,\lambda)|A_\mu|\bar{B}(p_B)\rangle &= i\frac{2}{m_B - m_A}\epsilon_{\mu\nu\alpha\beta}\epsilon^{*\nu}_{(\lambda)} p_B^\alpha p^\beta A^{BA}(q^2), \\ \langle A(p,\lambda)|V_\mu|\bar{B}(p_B)\rangle &= -\Big\{(m_B - m_A)\epsilon^{(\lambda)*}_\mu V_1^{BA}(q^2) \\ &\quad - (\epsilon^{(\lambda)*}\cdot p_B)(p_B + p)_\mu \frac{V_2^{BA}(q^2)}{m_B - m_A} \\ &\quad - 2m_A \frac{\epsilon^*_{(\lambda)} p_B}{q^2} q^\mu [V_3^{BA}(q^2) \\ &\quad - V_0^{BA}(q^2)]\Big\}, \\ \langle P(p)|V_\mu|\bar{B}(p_B)\rangle &= \left[(p_B + p)_\mu - \frac{m_B^2 - m_P^2}{q^2} q_\mu\right] \\ &\quad \times F_1^{BP}(q^2) + \frac{m_B^2 - m_P^2}{q^2} q_\mu F_0^{BP}(q^2), \end{aligned} \tag{2.43}$$

where $q = p_B - p$, $V_3^{BA}(0) = V_0^{BA}(0)$, $F_1^{BP}(0) = F_0^{BP}(0)$ and

$$V_3^{BA}(q^2) = \frac{m_B - m_A}{2m_A} V_1^{BA}(q^2) - \frac{m_B + m_A}{2m_A} V_2^{BA}(q^2). \tag{2.44}$$

In the literature the decay constant and the form factors of the axial-vector mesons are often defined in different manner. For example, in [24] they are defined as[4]

$$\langle A(p,\lambda)|A_\mu|0\rangle = f_A m_A \epsilon^{(\lambda)*}_\mu, \tag{2.45}$$

$$\begin{aligned} \langle A(p,\lambda)|A_\mu|\bar{B}(p_B)\rangle &= -\frac{2}{m_B - m_A}\epsilon_{\mu\nu\alpha\beta}\epsilon^{*\nu}_{(\lambda)} p_B^\alpha p^\beta A^{BA}(q^2), \\ \langle A(p,\lambda)|V_\mu|\bar{B}(p_B)\rangle &= -i\Big\{(m_B - m_A)\epsilon^{(\lambda)*}_\mu V_1^{BA}(q^2) \\ &\quad - (\epsilon^*_{(\lambda)} p_B)(p_B + p)_\mu \frac{V_2^{BA}(q^2)}{m_B - m_A} \\ &\quad - 2m_A \frac{\epsilon^*_{(\lambda)} p_B}{q^2} q^\mu \\ &\quad \times [V_3^{BA}(q^2) - V_0^{BA}(q^2)]\Big\}. \end{aligned} \tag{2.46}$$

It has been checked in the covariant light-front quark model that the form factors $V_{0,1,2}^{B^3P_1}(q^2)$ and $A^{B^3P_1}(q^2)$ defined in Eq. (2.46) are indeed positively defined. We would like to ask if the $\bar{B} \to {}^3P_1$ transition form factors defined in Eq. (2.43) are also positively defined. This can be checked by considering the factorizable amplitudes for the decay $\bar{B} \to AP$

$$\begin{aligned} X^{(\bar{B}A,P)} &= \langle P(q)|(V - A)_\mu|0\rangle\langle A(p)|(V - A)^\mu|\bar{B}(p_B)\rangle, \\ X^{(\bar{B}P,A)} &= \langle A(q)|(V - A)_\mu|0\rangle\langle P(p)|(V - A)^\mu|\bar{B}(p_B)\rangle. \end{aligned} \tag{2.47}$$

We obtain

$$\begin{aligned} X^{(\bar{B}A,P)} &= -2if_P m_A V_0^{BA}(q^2)(\epsilon^*_{(\lambda)} p_B), \\ X^{(\bar{B}P,A)} &= -2if_A m_A F_1^{BP}(q^2)(\epsilon^*_{(\lambda)} p_B), \end{aligned} \tag{2.48}$$

from Eqs. (2.12) and (2.43) and

$$\begin{aligned} X^{(\bar{B}A,P)} &= 2f_P m_A V_0^{BA}(q^2)(\epsilon^*_{(\lambda)} p_B), \\ X^{(\bar{B}P,A)} &= -2f_A m_A F_1^{BP}(q^2)(\epsilon^*_{(\lambda)} p_B), \end{aligned} \tag{2.49}$$

from Eqs. (2.45) and (2.46). Since f_A for the ${}^3P_1$ meson is negative in the light-front model calculation (see Eq. (2.23) and Table III in [24]), the relative sign between $X^{(\bar{B}A,P)}$ and $X^{(\bar{B}P,A)}$ is positive. This means that the relative sign in Eq. (2.48) is also positive provided that the decay constant f_A and the form factor V_0^{BA} defined in Eqs. (2.12) and (2.43), respectively, are of the same sign. Indeed, it is found in [16] that if f_A is chosen to be positive for the $a_1(1260)$ meson, the form factor $V_0^{Ba_1}$ is indeed positive according to the sum rule calculation.

The form factors for $B \to \pi$, K, $a_1(1260)$, $b_1(1235)$, K_{1A}, K_{1B} transitions have been calculated in the relativistic covariant light-front (CLF) quark model [24] (Table II)[5] and in the framework of the light cone sum rule (LCSR) approach [29]. In the CLF model, the momentum depen-

[4]Since the convention $\epsilon^{1234} = +1$ is adopted in [24] while $\epsilon_{1234} = +1$ is used in the present work, we have put an additional minus sign for the matrix element $\langle A(p,\lambda)|A_\mu|\bar{B}(p_B)\rangle$.

[5]As explained in the footnote before Eq. (2.2), we need to put additional minus signs to the $B \to {}^1P_1$ form factors in Table II since in the convention of the present work, the form factors $V_i^{B\to{}^1P_1}$ and $V_i^{B\to{}^3P_1}$ have different signs.

TABLE II. Form factors for $B \to \pi$, K, $a_1(1260)$, $b_1(1235)$, K_{1A}, K_{1B} transitions obtained in the covariant light-front model [24] are fitted to the 3-parameter form Eq. (2.50) except for the form factor V_2 denoted by $*$ for which the fit formula Eq. (2.51) is used.

F	$F(0)$	$F(q^2_{\rm max})$	a	b	F	$F(0)$	$F(q^2_{\rm max})$	a	b
$F_1^{B\pi}$	0.25	1.16	1.73	0.95	$F_0^{B\pi}$	0.25	0.86	0.84	0.10
F_1^{BK}	0.35	2.17	1.58	0.68	F_0^{BK}	0.35	0.80	0.71	0.04
A^{Ba_1}	0.25	0.76	1.51	0.64	$V_0^{Ba_1}$	0.13	0.32	1.71	1.23
$V_1^{Ba_1}$	0.37	0.42	0.29	0.14	$V_2^{Ba_1}$	0.18	0.36	1.14	0.49
A^{Bb_1}	−0.10	−0.23	1.92	1.62	$V_0^{Bb_1}$	−0.39	−0.98	1.41	0.66
$V_1^{Bb_1}$	0.18	0.36	1.03	0.32	$V_2^{Bb_1}$	0.03*	−0.15*	2.13*	2.39*
$A^{BK_{1A}}$	0.26	0.69	1.47	0.59	$V_0^{BK_{1A}}$	0.14	0.31	1.62	1.14
$V_1^{BK_{1A}}$	0.39	0.42	0.21	0.16	$V_2^{BK_{1A}}$	0.17	0.30	1.02	0.45
$A^{BK_{1B}}$	−0.11	−0.25	1.88	1.53	$V_0^{BK_{1B}}$	−0.41	−0.99	1.40	0.64
$V_1^{BK_{1B}}$	−0.19	−0.35	0.96	0.30	$V_2^{BK_{1B}}$	0.05*	0.16*	1.78*	2.12*

dence of the physical form factors is determined by first fitting the form factors obtained in the spacelike region to a 3-parameter function in q^2 and then analytically continuing them to the timelike region. Some of the $V_2(q^2)$ form factors in $P \to A$ transitions are fitted to a different 3-parameter form so that the fit parameters are stable within the chosen q^2 range.

Except for the form factor V_2 to be discussed below, it is found in [24] that the momentum dependence of form factors in the spacelike region can be well parametrized and reproduced in the three-parameter form:

$$F(q^2) = \frac{F(0)}{1 - a(q^2/m_B^2) + b(q^2/m_B^2)^2}, \tag{2.50}$$

for $B \to M$ transitions. The parameters a, b and $F(0)$ are first determined in the spacelike region. We then employ this parametrization to determine the physical form factors at $q^2 \geq 0$. In practice, these parameters are generally insensitive to the q^2 range to be fitted except for the form factor $V_2(q^2)$ in $B \to {}^1P_1$ transitions. The corresponding parameters a and b are rather sensitive to the chosen range for q^2. This sensitivity is attributed to the fact that the form factor $V_2(q^2)$ approaches to zero at very large $-|q^2|$ where the three-parameter parametrization (2.50) becomes questionable. To overcome this difficulty, we will fit this form factor to the form

$$F(q^2) = \frac{F(0)}{(1 - q^2/m_B^2)[1 - a(q^2/m_B^2) + b(q^2/m_B^2)^2]} \tag{2.51}$$

and achieve a substantial improvement [24].

Momentum dependence of the form factors calculated using the LCSR method is not shown in Table III. Since the pseudoscalar mesons considered in the present work are the light pion and the kaon, the form-factor q^2 dependence can be neglected for our purposes.

In principle, the experimental measurements of $\bar{B}^0 \to a_1^+\pi^-$ and $\bar{B}^0 \to b_1^+\pi^-$ will enable us to test the form factors $V_0^{Ba_1}$ and $V_0^{Bb_1}$ respectively. There are several existing model calculations for $B \to a_1$ form factors: one in a quark-meson model (CQM) [30], one in the ISGW2 model [31], one in the light-front quark model [24] and two based on the QCD sum rule (QSR) [29,32]. Predictions in various models are summarized in Table IV and in general they are quite different. For example, $V_0^{Ba_1}(0)$ obtained in the quark-meson model, 1.20, is larger than the value of the sum-rule prediction in [32], 0.23 ± 0.05. If $a_1(1260)$ behaves as the scalar partner of the ρ meson, $V_0^{Ba_1}$ is expected to be

TABLE III. Form factors for $B \to a_1(1260)$, $b_1(1235)$, K_{1A}, K_{1B}, f_1, f_8, h_1, h_8 transitions at $q^2 = 0$ obtained in the framework of the light cone sum rule approach [29]. Uncertainties arise from the Borel window and the input parameters.

$V_0^{Ba_1}(0)$	$0.303^{+0.022}_{-0.035}$	$V_0^{Bb_1}(0)$	$-0.356^{+0.039}_{-0.033}$
$V_0^{BK_{1A}}(0)$	$0.316^{+0.048}_{-0.042}$	$V_0^{BK_{1B}}(0)$	$-0.360^{+0.030}_{-0.028}$
$V_0^{Bf_1}(0)$	$0.181^{+0.018}_{-0.021}$	$V_0^{Bh_1}(0)$	$-0.214^{+0.021}_{-0.012}$
$V_0^{Bf_8}(0)$	$0.124^{+0.015}_{-0.004}$	$V_0^{Bh_8}(0)$	$-0.158^{+0.016}_{-0.018}$

TABLE IV. $B \to a_1(1260)$ transition form factor $V_0^{Ba_1}$ at $q^2 = 0$ in various models, where the QSR1 is the traditional QCD sum rule approach and the QSR2 is the light cone sum rule approach.

	CLF [24]	ISGW2 [31]	CQM [30]	QSR1 [32]	QSR2 [29]
$V_0^{Ba_1}(0)$	0.13	1.01	1.20	0.23 ± 0.05	$0.303^{+0.022}_{-0.035}$

similar to $A_0^{B\rho}$, which is of order 0.28 at $q^2 = 0$ [24]. Indeed, the sum rule calculation by one of us (K.C.Y.) yields $V_0^{Ba_1} = 0.303^{+0.022}_{-0.035}$. Therefore, it appears to us that a magnitude of order unity for $V_0^{Ba_1}(0)$ as predicted by the ISGW2 model and CQM is very unlikely. The *BABAR* measurement of $\bar{B}^0 \to a_1^+ \pi^-$ [4] favors a value of $V_0^{Ba_1}(0) \approx 0.30$, which is very close the LCSR result shown in Table III.

Various $B \to A$ form factors also have been calculated in the Isgur-Scora-Grinstein-Wise (ISGW) model [31,33] based on the nonrelativistic constituent quark picture. As pointed out in [24], in general, the form factors at small q^2 in CLF and ISGW models agree within 40%. However, $F_0^{BD_0^*}(q^2)$ and $V_1^{BD_1^{1/2}}(q^2)$ have a very different q^2 behavior in these two models as q^2 increases. Relativistic effects are mild in $B \to D^{**}$ transitions but can manifest in heavy-to-light transitions at maximum recoil. For example, $V_0^{Ba_1}(0)$ is found to be 0.13 in the CLF model, while it is as big as 1.01 in the ISGW2 model.

D. Light cone distribution amplitudes

For an axial-vector meson, the chiral-even LCDAs are given by

$$\langle A(P,\lambda)|\bar{q}_1(y)\gamma_\mu\gamma_5 q_2(x)|0\rangle = im_A \int_0^1 du e^{i(upy+\bar{u}px)}\left\{p_\mu \frac{\epsilon^{(\lambda)*}z}{pz}\Phi_\parallel(u) + \epsilon^{(\lambda)*}_{\perp\mu} g_\perp^{(a)}(u)\right\}, \tag{2.52}$$

$$\langle A(P,\lambda)|\bar{q}_1(y)\gamma_\mu q_2(x)|0\rangle = -im_A \epsilon_{\mu\nu\rho\sigma}\epsilon^{*\nu}_{(\lambda)} p^\rho z^\sigma \int_0^1 du e^{i(upy+\bar{u}px)} \frac{g_\perp^{(v)}(u)}{4}, \tag{2.53}$$

with $u(\bar{u} = 1-u)$ being the momentum fraction carried by $q_1(\bar{q}_2)$, and the chiral-odd LCDAs read

$$\langle A(P,\lambda)|\bar{q}_1(y)\sigma_{\mu\nu}\gamma_5 q_2(x)|0\rangle = \int_0^1 du e^{i(upy+\bar{u}px)}\left\{(\epsilon^{(\lambda)*}_{\perp\mu}p_\nu - \epsilon^{(\lambda)*}_{\perp\nu}p_\mu)\Phi_\perp(u) + \frac{m_A^2\epsilon^{(\lambda)*}z}{(pz)^2}(p_\mu z_\nu - p_\nu z_\mu)h_\parallel^{(t)}(u)\right\}, \tag{2.54}$$

$$\langle A(P,\lambda)|\bar{q}_1(y)\gamma_5 q_2(x)|0\rangle = m_A^2\epsilon^{(\lambda)*}z \int_0^1 du e^{i(upy+\bar{u}px)} \frac{h_\parallel^{(p)}(u)}{2}. \tag{2.55}$$

Here, throughout the present discussion, we define $z \equiv y - x$ with $z^2 = 0$ and introduce the lightlike vector $p_\mu = P_\mu - m_A^2 z_\mu/(2Pz)$ with the meson's momentum $P^2 = m_A^2$. Moreover, the meson polarization vector ϵ_μ has been decomposed into longitudinal $(\epsilon^{(\lambda)*}_{\parallel\mu})$ and transverse $(\epsilon^{(\lambda)*}_{\perp\mu})$ *projections* defined as

$$\epsilon^{(\lambda)*}_{\parallel\mu} \equiv \frac{\epsilon^*_{(\lambda)}z}{Pz}\left(P_\mu - \frac{m_A^2}{Pz}z_\mu\right), \qquad \epsilon^{(\lambda)*}_{\perp\mu} = \epsilon^{(\lambda)*}_\mu - \epsilon^{(\lambda)*}_{\parallel\mu}, \tag{2.56}$$

respectively. The LCDAs $\Phi_\parallel$, $\Phi_\perp$ are of twist-2, and $g_\perp^{(v)}$, $g_\perp^{(a)}$, $h_\perp^{(t)}$, $h_\parallel^{(p)}$ of twist-3. Because of G-parity, $\Phi_\parallel$, $g_\perp^{(v)}$ and $g_\perp^{(a)}$ are symmetric (antisymmetric) with the replacement of $u \to 1-u$ for ${}^3P_1$ $({}^1P_1)$ states, whereas $\Phi_\perp$, $h_\parallel^{(t)}$ and $h_\parallel^{(p)}$ are antisymmetric (symmetric) in the SU(3) limit [18]. We restrict ourselves to two-parton LCDAs with twist-3 accuracy.

Assuming that the axial-vector meson moves along the z-axis, the derivation for the light cone projection operator of an axial-vector meson in the momentum space is in complete analogy to the case of the vector meson. We separate the longitudinal and transverse parts for the projection operator:

$$M^A_{\delta\alpha} = M^A_{\delta\alpha\parallel} + M^A_{\delta\alpha\perp}, \tag{2.57}$$

where only the longitudinal part is relevant in the present study and is given by

$$M^A_\parallel = -i\frac{1}{4}\frac{m_A(\epsilon^*_{(\lambda)}n_+)}{2}\not{n}_-\gamma_5\Phi_\parallel(u) - \frac{im_A}{4}\frac{m_A(\epsilon^*_{(\lambda)}n_+)}{2E} \times\left\{\frac{i}{2}\sigma_{\mu\nu}\gamma_5 n_-^\mu n_+^\nu h_\parallel^{(t)}(u) + iE\int_0^u dv(\Phi_\perp(v) - h_\parallel^{(t)}(v))\sigma_{\mu\nu}\gamma_5 n_-^\mu \frac{\partial}{\partial k_{\perp\nu}} - \gamma_5\frac{h_\parallel^{(p)}(u)}{2}\right\}\Big|_{k=up}, \tag{2.58}$$

with the momentum of the quark q_1 in the A meson being

$$k_1^\mu = uEn_-^\mu + k_\perp^\mu + \frac{k_\perp^2}{4uE}n_+^\mu, \tag{2.59}$$

for which E is the energy of the axial-vector meson and the term proportional to $k_\perp^2$ is negligible. Here, for simplicity, we introduce two lightlike vectors $n_-^\mu \equiv (1,0,0,-1)$ and $n_+^\mu \equiv (1,0,0,1)$. In general, the QCD factorization amplitudes can be recast to the form $\int_0^1 du\,\mathrm{Tr}(M^A_\parallel \cdots)$.

The LCDAs $\Phi^A_{\parallel,\perp}(u)$ can be expanded in terms of Gegenbauer polynomials of the form:

$$\Phi^A_{\parallel(\perp)}(u) = 6u\bar{u}f_A^{(\perp)}\left[a_0^{\parallel(\perp),A} + \sum_{i=1}^\infty a_i^{\parallel(\perp),A}C_i^{3/2}(2u-1)\right]. \tag{2.60}$$

where the relevant decay constants in the above equation will be specified later. In the following we will discuss the LCDAs of $^1P_1$ and $^3P_1$ states separately:

1. $^1P_1$ mesons

For the $\Phi_{\perp(\parallel)}^{^1P_1}(u)$, due to the G-parity, only terms with odd (even) Gegenbauer moments survive in the SU(3) limit. Hence, the normalization condition for the twist-2 LCDA $\Phi_\perp^{^1P_1}$ can be chosen as

$$\int_0^1 du \Phi_\perp^{^1P_1}(u) = f_{^1P_1}^\perp. \tag{2.61}$$

In the present work, we consider the approximation

$$\Phi_\perp^{^1P_1}(u) = f_{^1P_1}^\perp 6u\bar{u}\Big\{1 + 3a_1^{\perp,^1P_1}(2u-1) + a_2^{\perp,^1P_1}\tfrac{3}{2}[5(2u-1)^2-1]\Big\}. \tag{2.62}$$

Likewise, we take

$$\Phi_\parallel^{^1P_1}(u) = f_{^1P_1}^\perp 6u\bar{u}\Big\{a_0^{\parallel,^1P_1} + 3a_1^{\parallel,^1P_1}(2u-1) + a_2^{\parallel,^1P_1}\tfrac{3}{2}[5(2u-1)^2-1]\Big\}, \tag{2.63}$$

with the normalization condition

$$\int_0^1 du \Phi_\parallel^{^1P_1}(u) = f_{^1P_1}. \tag{2.64}$$

This normalization together with Eq. (2.52) leads to Eq. (2.12) for the definition of the $^1P_1$ meson decay constant. Equations (2.63) and (2.64) lead to the relation

$$f_{^1P_1} = f_{^1P_1}^\perp(\mu) a_0^{\parallel,^1P_1}(\mu). \tag{2.65}$$

The scale dependence of $f_{^1P_1}^\perp$ must be compensated by that of the Gegenbauer moment $a_0^{\parallel,^1P_1}$ to ensure the scale independence of $f_{^1P_1}$. In principle, we can also use the decay constant $f_{^1P_1}$ to construct the LCDA $\Phi_\parallel^{^1P_1}$. However, $f_{^1P_1}$ vanishes for the neutral $b_1(1235)$ and is very small for the charged $b_1(1235)$. This implies a vanishing or very small $\Phi_\parallel^{^1P_1}$ unless the Gegenbauer moments $a_i^{\parallel,^1P_1}$ are very large. Hence, it is more convenient to employ the nonvanishing decay constant $f_{^1P_1}^\perp$ to construct $\Phi_\parallel^{^1P_1}$. This is very similar to the scalar meson case where the twist-2 light cone distribution amplitude Φ_S is expressed in the form [34]

$$\Phi_S(x,\mu) = \bar{f}_S(\mu) 6x(1-x) \times \Big[B_0(\mu) + \sum_{m=1}^{\infty} B_m(\mu) C_m^{3/2}(2x-1)\Big], \tag{2.66}$$

with $\bar{f}_S$ being defined as $\langle S|\bar{q}_2 q_1|0\rangle = m_S \bar{f}_S$. Now $\Phi_\parallel^{^1P_1}$ can be recast to the form

$$\Phi_\parallel^{^1P_1}(u) = f_{^1P_1} 6u\bar{u}\Big\{1 + \mu_{^1P_1} \sum_{i=1}^{2} a_i^{\parallel,^1P_1} C_i^{3/2}(2u-1)\Big\}, \tag{2.67}$$

with $\mu_{^1P_1} = 1/a_0^{\parallel,^1P_1}$. For the neutral $b_1(1235)$, f_{b_1} vanishes and μ_{b_1} becomes divergent, but the combination $f_{b_1}\mu_{b_1}$ is finite [35]. Recall that for the scalar meson case, its LCDA also can be expressed in the form

$$\Phi_S(x,\mu) = f_S 6x(1-x)\Big[1 + \mu_S \sum_{m=1}^{\infty} B_m(\mu) C_m^{3/2}(2x-1)\Big], \tag{2.68}$$

where $\bar{f}_S = \mu_S f_S$ and the equation of motion leads to $\mu_S = m_S/(m_2(\mu) - m_1(\mu))$. However, unlike the case for scalar mesons, the decay constants $f_{^1P_1}^\perp$ and $f_{^1P_1}$ cannot be related by equations of motion.

When the three-parton distributions and terms proportional to the light quark masses are neglected, the twist-3 distribution amplitudes can be related to the twist-2 $\Phi_\perp(u)$ for the transversely polarized axial-vector meson by Wandzura-Wilczek relations [18]:

$$\begin{aligned} h_\parallel^{(t)}(v) &= (2v-1)\Big[\int_0^v \frac{\Phi_\perp(u)}{\bar{u}} du - \int_v^1 \frac{\Phi_\perp(u)}{u} du\Big] \equiv (2v-1)\Phi_a(v), \\ h_\parallel^{\prime(p)}(v) &= -2\Big[\int_0^v \frac{\Phi_\perp(u)}{\bar{u}} du - \int_v^1 \frac{\Phi_\perp(u)}{u} du\Big] = -2\Phi_a(v), \\ \int_0^v du(\Phi_\perp(u) - h_\parallel^{(t)}(u)) &= v\bar{v}\Big[\int_0^v \frac{\Phi_\perp(u)}{\bar{u}} du - \int_v^1 \frac{\Phi_\perp(u)}{u} du\Big] = v\bar{v}\Phi_a(v). \end{aligned} \tag{2.69}$$

The twist-3 LCDA $\Phi_a(u,\mu)$ satisfies the normalization

$$\int_0^1 \Phi_a(u) du = 0, \tag{2.70}$$

and has the general expression

$$\Phi_a^{^1P_1}(u) = 3f_{^1P_1}^{\perp}\left[(2u-1) + \sum_{n=1}^{\infty} a_n^{\perp,^1P_1}(\mu) P_{n+1}(2u-1)\right], \tag{2.71}$$

where $P_n(u)$ are the Legendre polynomials.

2. $^3P_1$ mesons

In analogue to the $^1P_1$ case, we consider the approximations:

$$\Phi_{\parallel}^{^3P_1}(u) = f_{^3P_1} 6u\bar{u}\Big\{1 + 3a_1^{\parallel,^3P_1}(2u-1) + a_2^{\parallel,^3P_1}\tfrac{3}{2}[5(2u-1)^2-1]\Big\}, \tag{2.72}$$

$$\Phi_{\perp}^{^3P_1}(u) = f_{^3P_1} 6u\bar{u}\Big\{a_0^{\perp,^3P_1} + 3a_1^{\perp,^3P_1}(2u-1) + a_2^{\perp,^3P_1}\tfrac{3}{2}[5(2u-1)^2-1]\Big\}. \tag{2.73}$$

In the SU(3) limit, only terms with even (odd) Gegenbauer moments for $\Phi_{\parallel(\perp)}^{^3P_1}$ survive due to the G-parity. Hence, $a_1^{\parallel,^3P_1}$ and $a_{0,2}^{\perp,^3P_1}$ vanish in the SU(3) limit. The LCDAs respect the normalization conditions

$$\int_0^1 du\Phi_{\parallel}^{^3P_1}(u) = f_{^3P_1}, \qquad \int_0^1 du\Phi_{\perp}^{^3P_1}(u) = f_{^3P_1}^{\perp}, \tag{2.74}$$

and

$$\int_0^1 du h_{\parallel}^{(t)}(u) = \int_0^1 du h_{\parallel}^{(p)}(u) = 0. \tag{2.75}$$

The latter is valid in the SU(3) limit. Therefore, we obtain

$$f_{^3P_1}^{\perp}(\mu) = f_{^3P_1} a_0^{\perp,^3P_1}(\mu), \tag{2.76}$$

and

$$\Phi_{\perp}^{^3P_1}(u) = f_{^3P_1}^{\perp} 6u\bar{u}\Big\{1 + \mu_{^3P_1}\sum_{i=1}^{2} a_i^{\perp,^3P_1} C_i^{3/2}(2u-1)\Big\}, \tag{2.77}$$

with $\mu_{^3P_1} = 1/a_0^{\perp,^3P_1}$. The twist-3 LCDA Φ_a has the expression

$$\Phi_a^{^3P_1}(u,\mu) = 3f_{^3P_1}\Big[a_0^{\perp,^3P_1}(2u-1) + \sum_{n=1}^{\infty} a_n^{\perp,^3P_1}(\mu) P_{n+1}(2u-1)\Big]. \tag{2.78}$$

Most of the relevant Gegenbauer moments $a_i^{\parallel(\perp),A}$ have been evaluated using the QCD sum rule method [18]. The results are summarized in Table V.

For the pseudoscalar meson LCDAs we use

$$\Phi_P(u) = f_P 6u\bar{u}\Big\{1 + 3a_1^P(2u-1) + a_2^P\frac{3}{2}[5(2u-1)^2-1]\Big\},$$
$$\Phi_p(u) = f_P, \qquad \frac{\Phi_\sigma(u)}{6} = f_P u(1-u), \tag{2.79}$$

where Φ_p and Φ_σ are twist-3 LCDAs. We shall employ the sum rule results for the Gegenbauer moments of pseudoscalar mesons [36]

TABLE V. Gegenbauer moments of $\Phi_\perp$ and $\Phi_\parallel$ for 1^3P_1 and 1^1P_1 mesons, respectively, taken from [18].

μ	$a_2^{\parallel,a_1(1260)}$	$a_2^{\parallel,f_1^{^3P_1}}$	$a_2^{\parallel,f_8^{^3P_1}}$	$a_2^{\parallel,K_{1A}}$	$a_1^{\parallel,K_{1A}}$
1 GeV	-0.02 ± 0.02	-0.04 ± 0.03	-0.07 ± 0.04	-0.05 ± 0.03	0.00 ± 0.26
2.2 GeV	-0.01 ± 0.01	-0.03 ± 0.02	-0.05 ± 0.03	-0.04 ± 0.02	0.00 ± 0.22

μ	$a_1^{\perp,a_1(1260)}$	$a_1^{\perp,f_1^{^3P_1}}$	$a_1^{\perp,f_8^{^3P_1}}$	$a_1^{\perp,K_{1A}}$	$a_0^{\perp,K_{1A}}$	$a_2^{\perp,K_{1A}}$
1 GeV	-1.04 ± 0.34	-1.06 ± 0.36	-1.11 ± 0.31	-1.08 ± 0.48	0.08 ± 0.09	0.02 ± 0.20
2.2 GeV	-0.83 ± 0.27	-0.84 ± 0.29	-0.90 ± 0.25	-0.88 ± 0.39	0.07 ± 0.08	0.01 ± 0.15

μ	$a_1^{\parallel,b_1(1235)}$	$a_1^{\parallel,h_1^{^1P_1}}$	$a_1^{\parallel,h_8^{^3P_1}}$	$a_1^{\parallel,K_{1B}}$	$a_0^{\parallel,K_{1B}}$	$a_2^{\parallel,K_{1B}}$
1 GeV	-1.95 ± 0.35	-2.00 ± 0.35	-1.95 ± 0.35	-1.95 ± 0.45	0.14 ± 0.15	0.02 ± 0.10
2.2 GeV	-1.61 ± 0.29	-1.65 ± 0.29	-1.61 ± 0.29	-1.57 ± 0.37	0.14 ± 0.15	0.01 ± 0.07

μ	$a_2^{\perp,b_1(1235)}$	$a_2^{\perp,h_1^{^1P_1}}$	$a_2^{\perp,h_8^{^1P_1}}$	$a_2^{\perp,K_{1B}}$	$a_1^{\perp,K_{1B}}$
1 GeV	0.03 ± 0.19	0.18 ± 0.22	0.14 ± 0.22	-0.02 ± 0.22	0.17 ± 0.22
2.2 GeV	0.02 ± 0.15	0.14 ± 0.17	0.11 ± 0.17	-0.02 ± 0.17	0.14 ± 0.18

$$\begin{aligned}
&\mu = 1.0\ \text{GeV}: a_1^K = 0.06 \pm 0.03, \quad a_2^K = 0.25 \pm 0.15, \quad a_1^\pi = 0, \quad a_2^\pi = 0.25 \pm 0.15,\\
&\mu = 2.1\ \text{GeV}: a_1^K = 0.05 \pm 0.02, \quad a_2^K = 0.17 \pm 0.10, \quad a_1^\pi = 0, \quad a_2^\pi = 0.17 \pm 0.10.
\end{aligned} \tag{2.80}$$

Note that in this paper the G-parity violating parameters (a_1^K, $a_1^{\parallel,K_{1A}}$, $a_{0,2}^{\perp,K_{1A}}$, $a_1^{\perp,K_{1B}}$ and $a_{0,2}^{\parallel,K_{1B}}$) are for mesons containing a strange quark. For mesons involving an antistrange quark, the signs of G-parity violating parameters have to be flipped due to the G-parity. The integral of the B meson wave function is parametrized as [37]

$$\int_0^1 \frac{d\rho}{1-\rho}\Phi_1^B(\rho) \equiv \frac{m_B}{\lambda_B}, \tag{2.81}$$

where $1-\rho$ is the momentum fraction carried by the light spectator quark in the B meson. Here we use $\lambda_B(1\ \text{GeV}) = (350 \pm 100)$ MeV.

E. Other input parameters

For the CKM matrix elements, we use the Wolfenstein parameters $A = 0.818$, $\lambda = 0.22568$, $\bar{\rho} = 0.141$, and $\bar{\eta} = 0.348$ [38]. The corresponding three unitarity angles are $\alpha = 90.0°$, $\beta = 22.1°$ and $\gamma = 68.0°$.

For the running quark masses we shall use

$$\begin{aligned}
&m_b(m_b) = 4.2\ \text{GeV}, \quad m_b(2.1\ \text{GeV}) = 4.95\ \text{GeV}, \quad m_b(1\ \text{GeV}) = 6.89\ \text{GeV},\\
&m_c(m_b) = 1.3\ \text{GeV}, \quad m_c(2.1\ \text{GeV}) = 1.51\ \text{GeV}, \quad m_s(2.1\ \text{GeV}) = 90\ \text{MeV},\\
&m_s(1\ \text{GeV}) = 119\ \text{MeV}, \quad m_d(1\ \text{GeV}) = 6.3\ \text{MeV}, \quad m_u(1\ \text{GeV}) = 3.5\ \text{MeV}.
\end{aligned} \tag{2.82}$$

The uncertainty of the strange quark mass is assigned to be $m_s(2.1\ \text{GeV}) = 90 \pm 20$ MeV.

III. $B \to AP$ DECAYS IN QCD FACTORIZATION

We shall use the QCD factorization approach [37,39] to study the short-distance contributions to the $B \to AP$ decays with $A = a_1(1260)$, $f_1(1285)$, $f_1(1420)$, $K_1(1270)$, $b_1(1235)$, $h_1(1170)$, $h_1(1380)$, $K_1(1400)$, and $P = \pi$, K. It should be stressed that in order to define the LCDAs of axial-vector mesons properly, it is necessary to include the decay constants. However, for practical calculations, it is more convenient to factor out the decay constants in the LCDAs and put them back in the appropriate places. Recall that $\Phi_\parallel^{^1P_1}$ has two equivalent expressions, namely, Eqs. (2.63) and (2.67). However, we found out that it is most convenient to use Eq. (2.63) for the LCDA $\Phi_\parallel^{^1P_1}$ which amounts to treating the axial-vector decay constant of $^1P_1$ as $f_{^1P_1}^\perp$. (Of course, this does not mean that $f_{^1P_1}$ is equal to $f_{^1P_1}^\perp$.) Likewise, we shall use Eq. (2.77) rather than Eq. (2.73) for the LCDA $\Phi_\perp^{^3P_1}$.

In QCD factorization, the factorizable amplitudes of above-mentioned decays are collected in the appendix. They are expressed in terms of the flavor operators a_i^p and the annihilation operators b_i^p with $p = u$, c which can be calculated in the QCD factorization approach [37]. The flavor operators a_i^p are basically the Wilson coefficients in conjunction with short-distance nonfactorizable corrections such as vertex corrections and hard spectator interactions. In general, they have the expressions [37,39]

$$\begin{aligned}
a_i^p(M_1M_2) = &\left(c_i + \frac{c_{i\pm1}}{N_c}\right)N_i(M_2)\int_0^1 \Phi_\parallel^{M_2}(x)dx\\
&+ \frac{c_{i\pm1}}{N_c}\frac{C_F\alpha_s}{4\pi}\left[V_i(M_2) + \frac{4\pi^2}{N_c}H_i(M_1M_2)\right]\\
&+ P_i^p(M_2),
\end{aligned} \tag{3.1}$$

where $i = 1, \cdots, 10$, the upper (lower) signs apply when i is odd (even), c_i are the Wilson coefficients, $C_F = (N_c^2 - 1)/(2N_c)$ with $N_c = 3$, M_2 is the emitted meson and M_1 shares the same spectator quark with the B meson. The quantities $V_i(M_2)$ account for vertex corrections, $H_i(M_1M_2)$ for hard spectator interactions with a hard gluon exchange between the emitted meson and the spectator quark of the B meson and $P_i(M_2)$ for penguin contractions. The expression of the quantities $N_i(M_2)$ reads

$$N_i(M_2) = \begin{cases} 0 & i = 6, 8 \quad \text{and} \quad M_2 = A,\\ 1 & \text{else.}\end{cases} \tag{3.2}$$

Note that $N_i(M_2)$ vanishes for $i = 6$, 8 and $M_2 = A$ as a consequence of Eq. (2.70). The subscript $\parallel$ of Φ in the first term of Eq. (3.1) reminds us of the fact that it is the longitudinal component of the axial-vector meson's LCDA that contributes to the $B \to AP$ decay amplitude. Specifically, we have

$$\int_0^1 du\Phi_\parallel^{^1P_1}(u) = a_0^{\parallel,^1P_1}, \qquad \int_0^1 du\Phi_\parallel^{^3P_1}(u) = 1, \tag{3.3}$$

where we have factored out the decay constant $f_{^1P_1}^\perp$ ($f_{^3P_1}$) of $\Phi_\parallel^{^1P_1}$ ($\Phi_\parallel^{^3P_1}$).

The vertex corrections in Eq. (3.1) are given by

$$V_i(M_2) = \begin{cases} \int_0^1 dx \Phi_{M_2}(x)[12\ln\frac{m_b}{\mu} - 18 + g(x)]; & (i = 1-4, 9, 10), \\ \int_0^1 dx \Phi_{M_2}[-12\ln\frac{m_b}{\mu} + 6 - g(1-x)]; & (i = 5, 7), \\ \int_0^1 dx \Phi_{m_2}(x)[-6 + h(x)]; & (i = 6, 8), \end{cases} \tag{3.4}$$

with

$$\begin{aligned} g(x) &= 3\left(\frac{1-2x}{1-x}\ln x - i\pi\right) + \left[2\mathrm{Li}_2(x) - \ln^2 x + \frac{2\ln x}{1-x} - (3+2i\pi)\ln x - (x \leftrightarrow 1-x)\right], \\ h(x) &= 2\mathrm{Li}_2(x) - \ln^2 x - (1+2i\pi)\ln x - (x \leftrightarrow 1-x), \end{aligned} \tag{3.5}$$

where Φ_M (Φ_m) is the twist-2 (twist-3) light cone distribution amplitude of the meson M. More specifically, $\Phi_M = \Phi_P$, $\Phi_m = \Phi_p$ for $M = P$ and $\Phi_M = \Phi_\parallel^A$, $\Phi_m = \Phi_a$ for $M = A$. For the general LCDAs

$$\begin{aligned} \Phi_M(x) &= 6x(1-x)\left[\alpha_0 + \sum_{n=1}^{\infty}\alpha_n(\mu)C_n^{3/2}(2x-1)\right], \\ \Phi_m(x) &= \beta_0 + \sum_{n=1}^{\infty}\beta_n(\mu)P_n(2x-1), \end{aligned} \tag{3.6}$$

the vertex corrections read

$$\begin{aligned} V_i(M) = &\left(12\ln\frac{m_b}{\mu} - 18 - \frac{1}{2} - 3i\pi\right)\alpha_0 + \left(\frac{11}{2} - 3i\pi\right)\alpha_1 \\ &- \frac{21}{20}\alpha_2 + \left(\frac{79}{36} - \frac{2i\pi}{3}\right)\alpha_3 + \cdots, \end{aligned} \tag{3.7}$$

for $i = 1-4, 9, 10$,

$$\begin{aligned} V_i(M) = &\left(-12\ln\frac{m_b}{\mu} + 6 + \frac{1}{2} + 3i\pi\right)\alpha_0 + \left(\frac{11}{2} - 3i\pi\right)\alpha_1 \\ &+ \frac{21}{20}\alpha_2 + \left(\frac{79}{36} + \frac{2i\pi}{3}\right)\alpha_3 + \cdots, \end{aligned} \tag{3.8}$$

for $i = 5, 7$,

$$V_i(M) = -6\beta_0 + (3 - i2\pi)\beta_1 + \left(\frac{19}{18} - \frac{i\pi}{3}\right)\beta_3 + \cdots, \tag{3.9}$$

for $i = 6, 8$.

As for the hard spectator function H, it has the expression

$$\begin{aligned} H_i(M_1M_2) = &\frac{-if_Bf_{M_1}f_{M_2}}{X^{(\bar{B}M_1,M_2)}}\int_0^1\frac{d\rho}{\rho}\Phi_B(\rho)\int_0^1\frac{d\xi}{\bar{\xi}}\Phi_{M_2}(\xi) \\ &\times\int_0^1\frac{d\eta}{\bar{\eta}}\left[\Phi_{M_1}(\eta) \pm r_\chi^{M_1}\frac{\bar{\xi}}{\xi}\Phi_{m_1}(\eta)\right], \end{aligned} \tag{3.10}$$

for $i = 1-4, 9, 10$, where the upper sign is for $M_1 = P$ and the lower sign for $M_1 = A$,

$$\begin{aligned} H_i(M_1M_2) = &\frac{if_Bf_{M_1}f_{M_2}}{X^{(\bar{B}M_1,M_2)}}\int_0^1\frac{d\rho}{\rho}\Phi_B(\rho)\int_0^1\frac{d\xi}{\xi}\Phi_{M_2}(\xi) \\ &\times\int_0^1\frac{d\eta}{\bar{\eta}}\left[\Phi_{M_1}(\eta) \pm r_\chi^{M_1}\frac{\xi}{\bar{\xi}}\Phi_{m_1}(\eta)\right], \end{aligned} \tag{3.11}$$

for $i = 5, 7$ and $H_i = 0$ for $i = 6, 8$, $\bar{\xi} \equiv 1 - \xi$ and $\bar{\eta} \equiv 1 - \eta$. In the above equations,

$$r_\chi^P = \frac{2m_P^2}{m_b(\mu)(m_2 + m_1)(\mu)}, \qquad r_\chi^A = \frac{2m_A}{m_b(\mu)}, \tag{3.12}$$

and $X^{(\bar{B}M_1,M_2)}$ is the factorizable amplitude defined in Eq. (2.47).

Weak annihilation contributions are described by the terms b_i, and $b_{i,\mathrm{EW}}$ in Eq. (A1) which have the expressions

$$\begin{aligned} b_1 &= \frac{C_F}{N_c^2}c_1A_1^i, \\ b_3 &= \frac{C_F}{N_c^2}[c_3A_1^i + c_5(A_3^i + A_3^f) + N_cc_6A_3^f], \\ b_2 &= \frac{C_F}{N_c^2}c_2A_1^i, \\ b_4 &= \frac{C_F}{N_c^2}[c_4A_1^i + c_6A_2^f], \\ b_{3,\mathrm{EW}} &= \frac{C_F}{N_c^2}[c_9A_1^i + c_7(A_3^i + A_3^f) + N_cc_8A_3^i], \\ b_{4,\mathrm{EW}} &= \frac{C_F}{N_c^2}[c_{10}A_1^i + c_8A_2^i], \end{aligned} \tag{3.13}$$

where the subscripts 1, 2, 3 of $A_n^{i,f}$ denote the annihilation amplitudes induced from $(V-A)(V-A)$, $(V-A)(V+A)$, and $(S-P)(S+P)$ operators, respectively, and the superscripts i and f refer to gluon emission from the initial and final-state quarks, respectively. Their explicit expressions are:

$$
\begin{aligned}
A_1^i &= \int \cdots \begin{cases} (\Phi_P(x)\Phi_A(y)[\frac{1}{y(1-x\bar{y})} + \frac{1}{\bar{x}^2 y}] - r_\chi^A r_\chi^P \Phi_p(x)\Phi_a(y)\frac{2}{\bar{x}y}); & \text{for } M_1M_2 = AP, \\ (\Phi_A(x)\Phi_P(y)[\frac{1}{y(1-x\bar{y})} + \frac{1}{\bar{x}^2 y}] - r_\chi^A r_\chi^P \Phi_a(x)\Phi_p(y)\frac{2}{\bar{x}y}); & \text{for } M_1M_2 = PA, \end{cases} \\
A_2^i &= \int \cdots \begin{cases} (\Phi_P(x)\Phi_A(y)[\frac{1}{\bar{x}(1-x\bar{y})} + \frac{1}{\bar{x}y^2}] - r_\chi^A r_\chi^P \Phi_p(x)\Phi_a(y)\frac{2}{\bar{x}y}); & \text{for } M_1M_2 = AP, \\ (\Phi_A(x)\Phi_P(y)[\frac{1}{\bar{x}(1-x\bar{y})} + \frac{1}{\bar{x}y^2}] - r_\chi^A r_\chi^P \Phi_a(x)\Phi_p(y)\frac{2}{\bar{x}y}); & \text{for } M_1M_2 = PA, \end{cases} \\
A_3^i &= \int \cdots \begin{cases} (-r_\chi^A \Phi_P(x)\Phi_a(y)\frac{2\bar{y}}{\bar{x}y(1-x\bar{y})} - r_\chi^P \Phi_p(x)\Phi_A(y)\frac{2x}{\bar{x}y(1-x\bar{y})}); & \text{for } M_1M_2 = AP, \\ (r_\chi^P \Phi_A(x)\Phi_p(y)\frac{2\bar{y}}{\bar{x}y(1-x\bar{y})} + r_\chi^A \Phi_a(x)\Phi_P(y)\frac{2x}{\bar{x}y(1-x\bar{y})}); & \text{for } M_1M_2 = PA, \end{cases} \\
A_3^f &= \int \cdots \begin{cases} (-r_\chi^A \Phi_P(x)\Phi_a(y)\frac{2(1+\bar{x})}{\bar{x}^2 y} + r_\chi^P \Phi_p(x)\Phi_A(y)\frac{2(1+y)}{\bar{x}y^2}); & \text{for } M_1M_2 = AP, \\ (r_\chi^P \Phi_A(x)\Phi_p(y)\frac{2(1+\bar{x})}{\bar{x}^2 y} - r_\chi^A \Phi_a(x)\Phi_P(y)\frac{2(1+y)}{\bar{x}y^2}); & \text{for } M_1M_2 = PA, \end{cases} \\
A_1^f &= A_2^f = 0,
\end{aligned}
\tag{3.14}
$$

where $\int \cdots = \pi\alpha_s \int_0^1 dxdy$, $\bar{x} = 1 - x$, and $\bar{y} = 1 - y$. Note that we have adopted the same convention as in [39] that M_1 contains an antiquark from the weak vertex with longitudinal fraction $\bar{y}$, while M_2 contains a quark from the weak vertex with momentum fraction x.

Using the asymptotic distribution amplitudes for Φ_P, Φ_p, $\Phi_\parallel^{^3P_1}$, $\Phi_a^{^1P_1}$ and the leading contributions to $\Phi_\parallel^{^1P_1}$, $\Phi_a^{^3P_1}$:

$$
\begin{aligned}
&\Phi_P(u) = 6u\bar{u}, \qquad \Phi_\parallel^{^3P_1}(u) = 6u\bar{u}, \qquad \Phi_\parallel^{^1P_1}(u) = 18a_1^{\parallel,{}^1P_1} u\bar{u}(2u-1), \qquad \Phi_p(u) = 1, \\
&\Phi_a^{^3P_1}(u) = 3a_1^{\perp,{}^3P_1}(6u^2 - 6u + 1), \qquad \Phi_a^{^1P_1}(u) = 3(2u-1),
\end{aligned}
\tag{3.15}
$$

we obtain from Eq. (3.14) that

$$
\begin{aligned}
A_1^i({}^3P_1P) &\approx 6\pi\alpha_s\left[3\left(X_A - 4 + \frac{\pi^2}{3}\right) - a_1^{\perp,{}^3P_1} r_\chi^{^3P_1} r_\chi^P X_A(X_A - 3)\right], \\
A_1^i({}^1P_1P) &\approx 6\pi\alpha_s\left[-3a_1^{\parallel,{}^1P_1}(X_A + 29 - 3\pi^2) + r_\chi^{^1P_1} r_\chi^P X_A(X_A - 2)\right], \\
A_2^i({}^3P_1P) &\approx 6\pi\alpha_s\left[3\left(X_A - 4 + \frac{\pi^2}{3}\right) - a_1^{\perp,{}^3P_1} r_\chi^{^1P_1} r_\chi^P X_A(X_A - 3)\right], \\
A_2^i({}^1P_1P) &\approx 6\pi\alpha_s\left[-3a_1^{\parallel,{}^1P_1}(3X_A + 4 - \pi^2) + r_\chi^{^1P_1} r_\chi^P X_A(X_A - 2)\right], \\
A_3^i({}^3P_1P) &\approx 6\pi\alpha_s\left[-r_\chi^P\left(X_A^2 - 2X_A + \frac{\pi^2}{3}\right) - 3a_1^{\perp,{}^3P_1} r_\chi^{^3P_1}\left(X_A^2 - 2X_A - 6 + \frac{\pi^2}{3}\right)\right], \\
A_3^i({}^1P_1P) &\approx 6\pi\alpha_s[3a_1^{\parallel,{}^1P_1} r_\chi^P(X_A^2 - 4X_A + 4 + \frac{\pi^2}{3}) + 3r_\chi^{^1P_1}\left(X_A^2 - 2X_A + 4 - \frac{\pi^2}{3}\right)\Big], \\
A_3^f({}^3P_1P) &\approx 6\pi\alpha_s(2X_A - 1)[r_\chi^P X_A - 3a_1^{\perp,{}^3P_1} r_\chi^{^3P_1}(X_A - 3)], \\
A_3^f({}^1P_1P) &\approx 6\pi\alpha_s[-a_1^{\parallel,{}^1P_1} r_\chi^P X_A(6X_A - 11) + 3r_\chi^{^1P_1}(2X_A - 1)(X_A - 2)],
\end{aligned}
\tag{3.16}
$$

and

$$
\begin{aligned}
&A_1^i(P^3P_1) = A_1^i({}^3P_1P), \qquad A_1^i(P^1P_1) = -A_2^i({}^1P_1P), \qquad A_2^i(P^3P_1) = A_2^i({}^3P_1P), \qquad A_2^i(P^1P_1) = -A_1^i({}^1P_1P), \\
&A_3^i(P^3P_1) = -A_3^i({}^3P_1P), \qquad A_3^i(P^1P_1) = A_3^i({}^1P_1P), \qquad A_3^f(P^3P_1) = A_3^f({}^3P_1P), \qquad A_3^f(P^1P_1) = -A_3^f({}^1P_1P),
\end{aligned}
\tag{3.17}
$$

where the logarithmic divergences occurred in weak annihilation are described by the variable X_A

$$
\int_0^1 \frac{du}{u} \to X_A, \qquad \int_0^1 \frac{\ln u}{u} \to -\frac{1}{2}X_A. \tag{3.18}
$$

Following [37], these variables are parametrized as

$$
X_A = \ln\left(\frac{m_B}{\Lambda_h}\right)(1 + \rho_A e^{i\phi_A}), \tag{3.19}
$$

with the unknown real parameters ρ_A and ϕ_A. Likewise,

the endpoint divergence X_H in the hard spectator contributions can be parameterized in a similar manner. Following [34,40], we adopt $\rho_{A,H} \leq 0.5$ and arbitrary strong phases $\phi_{A,H}$ with $\rho_{A,H} = 0$ by default.

Besides the penguin and annihilation contributions formally of order $1/m_b$, there may exist other power corrections which unfortunately cannot be studied in a systematical way as they are nonperturbative in nature. The so-called "charming penguin" contribution is one of the long-distance effects that have been widely discussed. The importance of this nonperturbative effect has also been conjectured to be justified in the context of soft-collinear effective theory [41]. More recently, it has been shown that such an effect can be incorporated in final-state interactions [42]. However, in order to see the relevance of the charming penguin effect to B decays into scalar resonances, we need to await more data with better accuracy.

IV. NUMERICAL RESULTS

A. Branching ratios

The calculated branching ratios for the decays $B \to A\pi$, AK with $A = a_1(1260)$, $b_1(1235)$, $K_1(1270)$, $K_1(1400)$, $f_1(1285)$, $f_1(1420)$, $h_1(1170)$, $h_1(1380)$ are collected in Tables VI, VII, and VIII. For $B \to A$ transition form factors we use those obtained by the sum rule approach, Table III. The theoretical errors correspond to the uncertainties due to variation of (i) the Gegenbauer moments (Table V), the axial-vector meson decay constants, (ii) the heavy-to-light form factors and the strange quark mass, and (iii) the wave function of the B meson characterized by the parameter λ_B, the power corrections due to weak annihilation and hard spectator interactions described by the parameters $\rho_{A,H}$, $\phi_{A,H}$, respectively. To obtain the errors shown in Tables VI, VII, and VIII, we first scan randomly the points in the allowed ranges of the above seven parameters in three separated groups: the first two, the second two and the last three, and then add errors in each group in quadrature.

1. $\bar{B} \to a_1\pi$, $a_1\bar{K}$ decays

From Table VI we see that the predictions for $\bar{B}^0 \to a_1^{\pm}\pi^{\mp}$ are in excellent agreement with the average of the *BABAR* and Belle measurements [2,3]. *BABAR* has also measured time-dependent CP asymmetries in the decays $\bar{B}^0 \to a_1^{\pm}\pi^{\mp}$ [4]. Using the measured parameter ΔC (see Sec. IV B), *BABAR* is able to determine the rates of $\bar{B}^0 \to a_1^+\pi^-$ and $\bar{B}^0 \to a_1^-\pi^+$ separately, as shown in Table VI. It is expected that the latter governed by the decay constant of

TABLE VI. Branching ratios (in units of 10^{-6}) for the decays $B \to a_1(1260)\pi$, $a_1(1260)K$, $b_1(1235)\pi$ and $b_1(1235)K$. The theoretical errors correspond to the uncertainties due to variation of (i) Gegenbauer moments, decay constants, (ii) quark masses, form factors, and (iii) λ_B, $\rho_{A,H}$, $\phi_{A,H}$, respectively. Other model predictions are also presented here for comparison. In [14], predictions are obtained for two different sets of form factors, denoted by I and II, respectively, corresponding to the mixing angles $\theta_{K_1} = 32°$ and $58°$ (see the text for more details).

Mode	CMV [15]	LNP(I)[14]	LNP(II)	This work	Expt. [2–7,10]
$\bar{B}^0 \to a_1^+\pi^-$	74.3	4.7	11.8	$9.1^{+0.2+2.2+1.7}_{-0.2-1.8-1.1}$	12.2 ± 4.5 [a]
$\bar{B}^0 \to a_1^-\pi^+$	36.7	11.1	12.3	$23.4^{+2.3+6.2+1.9}_{-2.2-5.5-1.3}$	21.0 ± 5.4 [a]
$\bar{B}^0 \to a_1^{\pm}\pi^{\mp}$	111.0	15.8	24.1	$32.5^{+2.5+8.4+3.6}_{-2.4-7.3-2.4}$	31.7 ± 3.7 [b]
$B^- \to a_1^0\pi^-$	43.2	3.9	8.8	$7.6^{+0.3+1.7+1.4}_{-0.3-1.3-1.0}$	$20.4 \pm 4.7 \pm 3.4$
$\bar{B}^0 \to a_1^0\pi^0$	0.27	1.1	1.7	$0.9^{+0.1+0.3+0.7}_{-0.1-0.2-0.3}$	
$B^- \to a_1^-\pi^0$	13.6	4.8	10.6	$14.4^{+1.4+3.5+2.1}_{-1.3-3.2-1.9}$	$26.4 \pm 5.4 \pm 4.1$
$\bar{B}^0 \to a_1^+K^-$	72.2	1.6	4.1	$18.3^{+1.0+14.2+21.1}_{-1.0-7.2-7.5}$	$16.3 \pm 2.9 \pm 2.3$
$\bar{B}^0 \to a_1^0\bar{K}^0$	42.3	0.5	2.5	$6.9^{+0.3+6.1+9.5}_{-0.3-2.9-3.2}$	
$B^- \to a_1^-\bar{K}^0$	84.1	2.0	5.2	$21.6^{+1.2+16.5+23.6}_{-1.1-8.5-11.9}$	$34.9 \pm 5.0 \pm 4.4$
$B^- \to a_1^0K^-$	43.4	1.4	2.8	$13.9^{+0.9+9.5+12.9}_{-0.9-5.1-4.9}$	
$\bar{B}^0 \to b_1^+\pi^-$	36.2	6.9	0.7	$11.2^{+0.3+2.8+2.2}_{-0.3-2.4-1.9}$	
$\bar{B}^0 \to b_1^-\pi^+$	4.4	≈ 0	≈ 0	$0.3^{+0.1+0.1+0.3}_{-0.0-0.1-0.1}$	
$\bar{B}^0 \to b_1^{\pm}\pi^{\mp}$	40.6	6.9	0.7	$11.4^{+0.4+2.9+2.5}_{-0.3-2.5-2.0}$	$10.9 \pm 1.2 \pm 0.9$
$\bar{B}^0 \to b_1^0\pi^0$	0.15	0.5	0.01	$1.1^{+0.2+0.1+0.2}_{-0.2-0.1-0.2}$	
$B^- \to b_1^-\pi^0$	4.2	4.8	0.5	$0.4^{+0.0+0.2+0.4}_{-0.0-0.1-0.2}$	
$B^- \to b_1^0\pi^-$	18.6	4.5	0.4	$9.6^{+0.3+1.6+2.5}_{-0.3-1.6-1.5}$	$6.7 \pm 1.7 \pm 1.0$
$\bar{B}^0 \to b_1^+K^-$	35.7	2.4	0.2	$12.1^{+1.0+9.7+12.3}_{-0.9-4.9-30.2}$	$7.4 \pm 1.0 \pm 1.0$
$\bar{B}^0 \to b_1^0\bar{K}^0$	19.3	4.1	0.4	$7.3^{+0.5+5.4+6.7}_{-0.5-2.8-6.5}$	
$B^- \to b_1^-\bar{K}^0$	41.5	3.0	0.3	$14.0^{+1.3+11.5+13.9}_{-1.2-5.9-8.3}$	
$B^- \to b_1^0K^-$	18.1	2.6	0.07	$6.2^{+0.5+5.0+6.4}_{-0.5-2.5-5.2}$	$9.1 \pm 1.7 \pm 1.0$

[a] *BABAR* data only [4]. [b] The average of *BABAR* [2] and Belle [3] data.

TABLE VII. Same as Table VI except for the decays $B \to K_1(1270)\pi$, $K_1(1270)K$, $K_1(1400)\pi$, and $K_1(1400)K$ for two different mixing angles $\theta_{K_1} = -37°$ and $-58°$ (in parentheses). In the framework of [14], only the $K_1^-(1400)\pi^0$ and $\bar{K}_1^0(1400)\pi^0$ modes depend on the mixing angle θ_{K_1}. Note that the results of [14,15] shown in the table are obtained for $\theta_{K_1} = 32°$ and $58°$ (in parentheses).

Mode	[15]	[14]	This work	Expt. [8]
$\bar{B}^0 \to K_1^-(1270)\pi^+$	4.3 (4.3)	7.6	$3.0^{+0.8+1.5+4.2}_{-0.6-0.9-1.4}$ $(2.7^{+0.6+1.3+4.4}_{-0.5-0.8-1.5})$	$12.0 \pm 3.1^{+9.3}_{-4.5} < 25.2$
$\bar{B}^0 \to \bar{K}_1^0(1270)\pi^0$	2.3 (2.1)	0.4	$1.0^{+0.0+0.6+1.7}_{-0.0-0.3-0.6}$ $(0.8^{+0.1+0.5+1.7}_{-0.1-0.3-0.6})$	
$B^- \to \bar{K}_1^0(1270)\pi^-$	4.7 (4.7)	5.8	$3.5^{+0.1+1.8+5.1}_{-0.1-1.1-1.9}$ $(3.0^{+0.2+0.1+2.7}_{-0.2-0.2-2.2})$	
$B^- \to K_1^-(1270)\pi^0$	2.5 (1.6)	4.9	$2.7^{+0.1+1.1+3.1}_{-0.1-0.7-1.0}$ $(2.5^{+0.1+1.0+3.2}_{-0.1-0.7-1.0})$	
$\bar{B}^0 \to K_1^-(1400)\pi^+$	2.3 (2.3)	4.0	$5.4^{+1.1+1.7+9.9}_{-1.0-1.3-2.8}$ $(2.2^{+1.1+0.7+2.6}_{-0.8-0.6-1.3})$	$16.7 \pm 2.6^{+3.5}_{-5.0} < 21.8$
$\bar{B}^0 \to \bar{K}_1^0(1400)\pi^0$	1.7 (1.6)	3.0 (1.7)	$2.9^{+0.3+0.7+5.5}_{-0.3-0.6-1.7}$ $(1.5^{+0.4+0.3+1.7}_{-0.3-0.3-0.9})$	
$B^- \to \bar{K}_1^0(1400)\pi^-$	2.5 (2.5)	3.0	$6.5^{+1.0+2.0+11.6}_{-0.9-1.6-3.6}$ $(2.8^{+1.0+0.9+3.0}_{-0.8-0.9-1.7})$	
$B^- \to K_1^-(1400)\pi^0$	0.7 (0.6)	1.0 (1.4)	$3.0^{+0.4+1.1+5.2}_{-0.4-0.7-1.3}$ $(1.0^{+0.4+0.4+1.2}_{-0.3-0.4-0.5})$	
$\bar{B}^0 \to K_1^-(1270)K^+$			$0.01^{+0.01+0.00+0.02}_{-0.00-0.00-0.01}$ $(0.01^{+0.00+0.00+0.02}_{-0.00-0.00-0.01})$	
$\bar{B}^0 \to K_1^+(1270)K^-$			$0.06^{+0.01+0.00+0.46}_{-0.01-0.00-0.06}$ $(0.04^{+0.01+0.00+0.27}_{-0.01-0.00-0.04})$	
$B^- \to K_1^0(1270)K^-$	0.22 (0.22)		$0.25^{+0.01+0.15+0.39}_{-0.01-0.08-0.09}$ $(0.22^{+0.01+0.12+0.39}_{-0.01-0.07-0.12})$	
$B^- \to K_1^-(1270)K^0$	0.02 (0.75)		$0.05^{+0.02+0.07+0.10}_{-0.02-0.03-0.04}$ $(0.05^{+0.02+0.09+0.10}_{-0.01-0.03-0.04})$	
$\bar{B}^0 \to \bar{K}_1^0(1270)K^0$	0.02 (0.70)		$2.30^{+0.16+1.13+1.43}_{-0.15-0.61-0.61}$ $(2.10^{+0.13+1.23+1.31}_{-0.13-0.65-0.57})$	
$\bar{B}^0 \to K_1^0(1270)\bar{K}^0$	0.20 (0.20)		$0.24^{+0.01+0.11+0.33}_{-0.01-0.07-0.13}$ $(0.26^{+0.10+0.12+0.47}_{-0.01-0.08-0.17})$	
$\bar{B}^0 \to K_1^-(1400)K^+$			$0.09^{+0.01+0.00+0.23}_{-0.01-0.00-0.09}$ $(0.07^{+0.02+0.00+0.16}_{-0.02-0.00-0.06})$	
$\bar{B}^0 \to K_1^+(1400)K^-$			$0.02^{+0.00+0.00+0.04}_{-0.00-0.00-0.00}$ $(0.01^{+0.00+0.00+0.16}_{-0.00-0.00-0.00})$	
$B^- \to K_1^0(1400)K^-$	0.12 (0.12)		$0.48^{+0.08+0.15+0.81}_{-0.08-0.12-0.26}$ $(0.22^{+0.07+0.07+0.24}_{-0.07-0.07-0.13})$	
$B^- \to K_1^-(1400)K^0$	4.4 (3.9)		$0.01^{+0.00+0.01+0.14}_{-0.00-0.00-0.01}$ $(0.01^{+0+0.02+0.04}_{-0-0.00-0.00})$	
$\bar{B}^0 \to \bar{K}_1^0(1400)K^0$	4.1 (3.6)		$0.08^{+0.01+0.17+0.59}_{-0.01-0.06-0.08}$ $(0.10^{+0.02+0.21+0.15}_{-0.02-0.08-0.10})$	
$\bar{B}^0 \to K_1^0(1400)\bar{K}^0$	0.11 (0.11)		$0.50^{+0.08+0.13+0.92}_{-0.07-0.11-0.32}$ $(0.25^{+0.07+0.08+0.31}_{-0.07-0.07-0.15})$	

TABLE VIII. Same as Table VI except for the decays $B \to f_1\pi$, f_1K, $h_1\pi$, and h_1K with $f_1 = f_1(1285)$, $f_1(1420)$ and $h_1 = h_1(1170)$, $h_1(1380)$. We use two different sets of mixing angles, namely, $\theta_{^3P_1} = 27.9°$ and $\theta_{^1P_1} = 25.2°$ (top), corresponding to $\theta_{K_1} = -37°$, and $\theta_{^3P_1} = 53.2°$, $\theta_{^1P_1} = -18.1°$ (bottom), corresponding to $\theta_{K_1} = -58°$.

Mode	Theory	Mode	Theory
$B^- \to f_1(1285)\pi^-$	$5.2^{+0.3+1.3+0.7}_{-0.2-1.0-0.2}$	$B^- \to f_1(1420)\pi^-$	$0.06^{+0.01+0.01+0.00}_{-0.00-0.00-0.00}$
$\bar{B}^0 \to f_1(1285)\pi^0$	$0.26^{+0.03+0.14+0.29}_{-0.03-0.07-0.08}$	$\bar{B}^0 \to f_1(1420)\pi^0$	$0.003^{+0.003+0.002+0.003}_{-0.002-0.001-0.002}$
$B^- \to f_1(1285)K^-$	$14.8^{+3.0+7.5+12.4}_{-2.6-3.9-5.2}$	$B^- \to f_1(1420)K^-$	$6.0^{+1.7+1.9+9.0}_{-1.5-1.3-3.1}$
$\bar{B}^0 \to f_1(1285)\bar{K}^0$	$14.6^{+2.7+7.5+11.9}_{-2.3-3.9-5.0}$	$\bar{B}^0 \to f_1(1420)\bar{K}^0$	$5.5^{+1.6+1.8+8.4}_{-1.3-1.2-2.8}$
$B^- \to h_1(1170)\pi^-$	$4.8^{+0.4+0.9+0.8}_{-0.3-0.8-0.7}$	$B^- \to h_1(1380)\pi^-$	$0.17^{+0.03+0.06+0.04}_{-0.02-0.06-0.03}$
$\bar{B}^0 \to h_1(1170)\pi^0$	$0.19^{+0.06+0.05+0.07}_{-0.04-0.03-0.01}$	$\bar{B}^0 \to h_1(1380)\pi^0$	$0.006^{+0.009+0.005+0.007}_{-0.004-0.004-0.002}$
$B^- \to h_1(1170)K^-$	$10.1^{+4.7+2.1+7.3}_{-3.1-1.4-8.1}$	$B^- \to h_1(1380)K^-$	$12.7^{+7.1+9.2+211.4}_{-5.1-4.7-10.8}$
$\bar{B}^0 \to h_1(1170)\bar{K}^0$	$10.1^{+4.2+2.2+7.2}_{-2.8-1.5-8.1}$	$\bar{B}^0 \to h_1(1380)\bar{K}^0$	$11.3^{+6.4+8.5+188.5}_{-4.6-4.3-9.6}$
$B^- \to f_1(1285)\pi^-$	$4.6^{+0.2+1.1+0.6}_{-0.2-0.9-0.2}$	$B^- \to f_1(1420)\pi^-$	$0.59^{+0.06+0.18+0.10}_{-0.05-0.13-0.05}$
$\bar{B}^0 \to f_1(1285)\pi^0$	$0.20^{+0.02+0.12+0.24}_{-0.02-0.06-0.06}$	$\bar{B}^0 \to f_1(1420)\pi^0$	$0.05^{+0.02+0.03+0.04}_{-0.01-0.02-0.02}$
$B^- \to f_1(1285)K^-$	$5.2^{+0.9+3.1+9.1}_{-0.8-1.5-10.0}$	$B^- \to f_1(1420)K^-$	$13.8^{+4.0+5.6+17.1}_{-3.3-3.2-6.3}$
$\bar{B}^0 \to f_1(1285)\bar{K}^0$	$5.2^{+0.8+3.2+3.0}_{-0.7-1.5-1.4}$	$\bar{B}^0 \to f_1(1420)\bar{K}^0$	$13.1^{+3.7+5.4+16.2}_{-3.0-3.1-5.9}$
$B^- \to h_1(1170)\pi^-$	$1.8^{+0.3+0.3+0.3}_{-0.2-0.3-0.3}$	$B^- \to h_1(1380)\pi^-$	$2.9^{+0.2+0.6+0.4}_{-0.1-0.6-0.4}$
$\bar{B}^0 \to h_1(1170)\pi^0$	$0.16^{+0.08+0.01+0.06}_{-0.05-0.01-0.04}$	$\bar{B}^0 \to h_1(1380)\pi^0$	$0.04^{+0.00+0.03+0.04}_{-0.00-0.02-0.01}$
$B^- \to h_1(1170)K^-$	$11.3^{+5.8+1.9+23.0}_{-3.7-1.1-8.2}$	$B^- \to h_1(1380)K^-$	$5.6^{+0.9+2.3+1.4}_{-0.7-1.2-1.9}$
$\bar{B}^0 \to h_1(1170)\bar{K}^0$	$10.9^{+5.3+1.9+21.1}_{-3.4-1.2-7.7}$	$\bar{B}^0 \to h_1(1380)\bar{K}^0$	$5.5^{+0.7+2.4+1.5}_{-0.7-1.2-2.0}$

$a_1(1260)$ has a rate larger than the former as $f_{a_1} \gg f_\pi$. Again, theory is consistent the data within errors. However, there are some discrepancies between theory and experiment for $a_1^0\pi^-$ and $a_1^-\pi^0$ modes. It appears that the relations $\mathcal{B}(B^- \to a_1^0\pi^-) \gtrsim \mathcal{B}(\bar{B}^0 \to a_1^+\pi^-)$ and $\mathcal{B}(B^- \to a_1^-\pi^0) \gtrsim \mathcal{B}(\bar{B}^0 \to a_1^-\pi^+)$ observed by *BABAR* are opposite to the naive expectation that $\mathcal{B}(B^- \to a_1^0\pi^-) < \mathcal{B}(\bar{B}^0 \to a_1^+\pi^-)$ and $\mathcal{B}(B^- \to a_1^-\pi^0) < \mathcal{B}(\bar{B}^0 \to a_1^-\pi^+)$. As for $B \to a_1 K$ decays, although the agreement with the data for $\bar{B}^0 \to a_1^+ K^-$ is excellent, the expectation of $\mathcal{B}(B^- \to a_1^-\bar{K}^0) \sim \mathcal{B}(\bar{B}^0 \to a_1^+ K^-)$ is not consistent with experiment. More specifically, in QCDF we obtain the ratios

$$\begin{aligned} R_1 &\equiv \frac{\mathcal{B}(B^- \to a_1^0\pi^-)}{\mathcal{B}(\bar{B}^0 \to a_1^+\pi^-)} = 0.83^{+0.02+0.06+0.12}_{-0.02-0.05-0.17} \qquad \text{(expt: } 1.67 \pm 0.78\text{)}, \\ R_2 &\equiv \frac{\mathcal{B}(B^- \to a_1^-\pi^0)}{\mathcal{B}(\bar{B}^0 \to a_1^-\pi^+)} = 0.62^{+0.01+0.01+0.08}_{-0.01-0.01-0.10} \qquad \text{(expt: } 1.26 \pm 0.46\text{)}, \\ R_3 &\equiv \frac{\mathcal{B}(B^- \to a_1^-\bar{K}^0)}{\mathcal{B}(\bar{B}^0 \to a_1^+ K^-)} = 1.18^{+0.01+0.02+0.04}_{-0.01-0.02-0.04} \qquad \text{(expt: } 2.14 \pm 0.63\text{)}. \end{aligned} \tag{4.1}$$

In the above ratios the hadronic uncertainties are mainly governed by weak annihilation and spectator scattering in R_1, R_2 and largely canceled out in R_3. It is evident that while the predicted R_1 is barely consistent with the data within errors, theory does not agree with experiment for R_2 and R_3. This should be clarified by the improved measurements of these modes in the future.

While the tree-dominated $a_1\pi$ modes have similar rates as $\rho\pi$ ones, the penguin-dominated $a_1 K$ modes resemble much more to πK than ρK, as first pointed out in [16]. One can see from Eqs. (A3) and (A7) that the dominant penguin coefficients $\alpha_4^p(a_1 K)$ and $\alpha_4^p(\pi K)$ are constructive in a_4^p and a_6^p penguin coefficients:

$$\begin{aligned} \alpha_4^p(a_1 K) &= a_4^p(a_1 K) + r_\chi^K a_6^p(a_1 K), \\ \alpha_4^p(\pi K) &= a_4^p(\pi K) + r_\chi^K a_6^p(\pi K), \end{aligned} \tag{4.2}$$

whereas $\alpha_4^p(\rho K) = a_4^p(\rho K) - r_\chi^K a_6^p(\rho K)$ [39]. Consequently, when the weak annihilation contribution is small, $B \to a_1 K$ and $B \to \pi K$ decays should have similar rates. However, if weak annihilation is important, then it will contribute more to the $a_1 K$ mode than the πK one due to the fact that $f_{a_1} \gg f_\pi$, recalling that the weak annihilation amplitude is proportional to $f_B f_{M_1} f_{M_2} b_i$. By comparing Table VI of the present work with Table 2 of [39], we see that the default results for the branching ratios of $B \to a_1 K$ and $B \to \pi K$ decays are indeed similar, while the hadronic uncertainties arising from weak annihilation are bigger in the former.

2. $\bar{B} \to b_1\pi$, $b_1\bar{K}$ decays

As for $\bar{B} \to b_1(1235)\pi$ decays, there is a good agreement between theory and experiment. Notice that it is naively expected that the $b_1^-\pi^+$ mode is highly suppressed relative to the $b_1^+\pi^-$ one as the decay amplitude of the former has the form $a_1 F_1^{B\pi} * f_{b_1}\Phi_\parallel^{b_1}$ (a_1 being the effective Wilson coefficient for the color-allowed tree amplitude) and the decay constant f_{b_1} vanishes in the isospin limit. As noted in passing, the LCDA $\Phi_\parallel^{b_1}(u)$ given by (2.67) is finite even if $f_{b_1} = 0$. This is because the coefficient $\mu_{b_1} = 1/a_0^{\parallel,b_1}$ in the wave function of b_1 will become divergent if $f_{b_1} = 0$, but the combination $f_{b_1}\mu_{b_1}$ is finite. More precisely, $f_{b_1}\mu_{b_1}$ is equal to $f_{b_1}^\perp$, the transverse decay constant of the b_1 [cf. Eq. (2.65)]. Therefore, $\Phi_\parallel^{b_1}(u)$ can be recast to the form of Eq. (2.63) which amounts to replacing f_{b_1} by $f_{b_1}^\perp$ in the calculation. Now, one may wonder how to see the suppression of $b_1^-\pi^+$ relative to $b_1^+\pi^-$? The key point is the term $\int \Phi_\parallel^M(x)dx$ appearing in the expression for the effective parameter a_i [see Eq. (3.1)]. This term vanishes for the b_1 meson in the isospin limit. As a result, the parameter a_1 for the decay $\bar{B}^0 \to b_1^-\pi^+$ vanishes in the absence of vertex, penguin, and spectator corrections. On the contrary, $a_1 = c_1 + \frac{c_2}{3} + \cdots$ for the channel $\bar{B}^0 \to b_1^+\pi^-$. This explains the suppression of $\bar{B}^0 \to b_1^-\pi^+$ relative to $b_1^+\pi^-$. After all, the $b_1^-\pi^+$ mode does not evade the decay constant suppression. It does receive contributions from vertex and hard spectator corrections and weak annihilation, but they are all suppressed. The *BABAR* measurement of charge-flavor asymmetry ΔC implies the ratio $\Gamma(\bar{B}^0 \to b_1^-\pi^+)/\Gamma(\bar{B}^0 \to b_1^\pm\pi^\mp) = -0.01 \pm 0.12$ [5]. This confirms the expected suppression.

Since $\bar{B} \to b_1\bar{K}$ decays receive sizable annihilation contributions, their rates are sensitive to the interference between penguin and annihilation terms. As a consequence, the measured branching ratios of $\bar{B} \to b_1\bar{K}$ would provide useful information on the sign of the $B \to b_1(1235)$ transition form factors. We found that if the form factor $V_0^{Bb_1}$ is of the same sign as $V_0^{Ba_1}$, $\mathcal{B}(\bar{B} \to b_1\bar{K})$ will be enhanced by a factor of $2 \sim 3$, for example, $\mathcal{B}(\bar{B}^0 \to b_1^+ K^-) \approx 21 \times 10^{-6}$ which is too large compared to the experimental value of $(7.4 \pm 1.4) \times 10^{-6}$ [5]. This means that the interference between penguin and annihilation contributions

should be *destructive* and the form factors $V_0^{Bb_1}$ and $V_0^{Ba_1}$ must be of opposite signs.

We also found that the naive relation $\mathcal{B}(B^- \to b_1^0 K^-) \sim \frac{1}{2}\mathcal{B}(\bar{B}^0 \to b_1^+ K^-)$ holds in QCDF. More precisely, QCDF predicts

$$R_4 \equiv \frac{\mathcal{B}(B^- \to b_1^0 K^-)}{\mathcal{B}(\bar{B}^0 \to b_1^+ K^-)} = 0.51^{+0.01+0.01+0.20}_{-0.01-0.00-0.02} \quad \text{(expt: } 1.23 \pm 0.36\text{)}, \tag{4.3}$$

where the hadronic uncertainty in R_4 arises almost entirely from weak annihilation (contribution from spectator scattering is negligible). This indicates that the data of $b_1^0 K^-$ and $b_1^+ K^-$ can be simultaneously explained only if the weak annihilation mechanism plays a dominant role in these decays.

3. $B \to K_1(1270)(\pi, K)$, $K_1(1400)(\pi, K)$ *decays*

It is evident from Table VII that the central values of the calculated branching ratios in QCDF for $K_1^-(1270)\pi^+$ and $K_1^-(1400)\pi^+$ are too small compared to experiment. This is not surprising as the same phenomenon also occurs in the penguin-dominated $B \to PV$ and $B \to VV$ decays. For example, the default results for the branching fractions of $B \to K^*\pi$ obtained in QCDF are in general too small by a factor of 2–3 compared to the data [39]. This suggests the importance of power corrections due to the nonvanishing ρ_A and ρ_H parameters or due to possible final-state rescattering effects from charm intermediate states [42]. It has been demonstrated in [39] that in the so-called "S4" scenario with $\rho_A = 1$ and nonvanishing ϕ_A, the global results for the VP modes agree better with the data. It has also been shown in [43] that the choice of $\rho_A e^{i\phi_A} = 0.6e^{-i40^\circ}$ will allow one to explain the polarization effects observed in various $B \to VV$ decays. While large power corrections from weak annihilation seem to be inevitable for explaining the $K_1\pi$ rates, one issue is that large weak annihilation may destroy the existing good agreement for $a_1^+ K^-$ and $b_1^+ K^-$ modes.

We notice that while $K_1(1270)\pi$ rates are insensitive to the mixing angle θ_{K_1}, the branching fractions of $K_1(1400)\pi$ are smaller for $\theta_{K_1} = -58^\circ$ than that for $\theta_{K_1} = -37^\circ$ by a factor of 2–3 due to the dependence of the $K_1(1400)$ decay constant on θ_{K_1}, recalling that $f_{K_1(1400)} \sim 112\ (235)$ MeV for $\theta_{K_1} = -58^\circ\ (-37^\circ)$ [cf. Eq. (2.32)]. The current measurement of $\bar{B}^0 \to K_1^-(1400)\pi^+$ favors a mixing angle of -37° over -58°.

Just as the case of $B \to KK^*$ decays, we find that the branching ratios of $B \to K_1(1270)K$ and $K_1(1400)K$ modes are of order $10^{-7} - 10^{-8}$ except for the decay $\bar{B}^0 \to \bar{K}_1^0(1270)K^0$ which can have a branching ratio of order 2.3×10^{-6}. The decay modes $K_1^- K^+$ and $K_1^+ K^-$ are of particular interest as they are the only AP modes which receive contributions solely from weak annihilation.

4. $B \to f_1(\pi, K)$, $h_1(\pi, K)$ *decays*

Branching ratios for the decays $B \to f_1\pi, f_1 K, h_1\pi$, and $h_1 K$ with $f_1 = f_1(1285)$, $f_1(1420)$ and $h_1 = h_1(1170)$, $h_1(1380)$ are shown in Table VIII for two different sets of mixing angles: (i) $\theta_{^3P_1} = 53.2^\circ$ and $\theta_{^1P_1} = -18.1^\circ$, corresponding to $\theta_{K_1} = -37^\circ$, and (ii) $\theta_{^3P_1} = 27.9^\circ$ and $\theta_{^1P_1} = 25.2^\circ$, corresponding to $\theta_{K_1} = -58^\circ$ (see Sec. II A).[6] Their branching ratios are naively expected to be of order $10^{-6} \sim 10^{-5}$ except for the color-suppressed $f_1\pi^0$ and $h_1\pi^0$ modes which are suppressed relative to the color-allowed one such as $f_1(1285)\pi^-$ by a factor of $|a_2/a_1|^2/2 \sim \mathcal{O}(0.03 - 0.08)$. However, an inspection of Table VIII shows some exceptions, for example, $\mathcal{B}(B^- \to f_1(1420)\pi^-) \ll \mathcal{B}(B^- \to f_1(1285)\pi^-)$ for both sets of $\theta_{^3P_1}$ and $\mathcal{B}(B^- \to h_1(1380)\pi^-) \ll \mathcal{B}(B^- \to h_1(1170)\pi^-)$ for $\theta_{^1P_1} = 25.2^\circ$. These can be understood as a consequence of interference. The decay amplitudes for the tree-dominated channels $h_1\pi^-$ are given by

$$\begin{aligned} A(B^- \to h_1(1380)\pi^-) &\propto -V_0^{Bh_1}\sin\theta_{^1P_1} + V_0^{Bh_8}\cos\theta_{^1P_1}, \\ A(B^- \to h_1(1170)\pi^-) &\propto V_0^{Bh_1}\cos\theta_{^1P_1} + V_0^{Bh_8}\sin\theta_{^1P_1}. \end{aligned} \tag{4.4}$$

Since the form factors $V_0^{Bh_1}$ and $V_0^{Bh_8}$ are of the same signs (cf. Table III), it is clear that the interference is constructive (destructive) in the $h_1(1170)\pi^-$ mode, but destructive (constructive) in $h_1(1380)\pi^-$ for $\theta_{^1P_1} = 25.2^\circ$ (-18.1°). This explains why $\mathcal{B}(B^- \to h_1(1380)\pi^-) \ll \mathcal{B}(B^- \to h_1(1170)\pi^-)$ for $\theta_{^1P_1} = 25.2^\circ$ and $\mathcal{B}(B^- \to h_1(1380)\pi^-) > \mathcal{B}(B^- \to h_1(1170)\pi^-)$ for $\theta_{^1P_1} = -18.1^\circ$. Therefore, a measurement of the ratio $R_5 \equiv \mathcal{B}(B^- \to h_1(1380)\pi^-)/\mathcal{B}(B^- \to h_1(1170)\pi^-)$ will help determine the mixing angle $\theta_{^1P_1}$. Likewise, information on the angle $\theta_{^3P_1}$ can be inferred from the ratio $R_6 \equiv \mathcal{B}(\bar{B} \to f_1(1420)\bar{K})/\mathcal{B}(\bar{B} \to f_1(1285)\bar{K})$: $R_6 > 1$ for $\theta_{^3P_1} = 53.2^\circ$ and $R_6 < 1$ for $\theta_{^3P_1} = 27.9^\circ$.

The preliminary *BABAR* results are [9]

$$\begin{aligned} &\mathcal{B}(B^- \to f_1(1285)K^-)\mathcal{B}(f_1(1285) \to \eta\pi\pi) \\ &\quad < 0.8 \times 10^{-6}, \\ &\mathcal{B}(B^- \to f_1(1420)K^-)\mathcal{B}(f_1(1420) \to \eta\pi\pi) \\ &\quad < 2.9 \times 10^{-6}, \\ &\mathcal{B}(B^- \to f_1(1420)K^-)\mathcal{B}(f_1(1420) \to K_S K^\pm \pi^\mp) \\ &\quad < 4.1 \times 10^{-6}. \end{aligned} \tag{4.5}$$

Since $\mathcal{B}(f_1(1285) \to \eta\pi\pi) = 0.52 \pm 0.16$ [1], the upper limit on $\mathcal{B}(B^- \to f_1(1285)K^-)$ is inferred to be of order

[6]There are predictions for the decay rates of $B \to f_1\pi$, $f_1 K$, $h_1\pi$, and $h_1 K$ in [15]. Since the f_1 and h_1 states are not specified there, we will not include them in Table VIII for comparison.

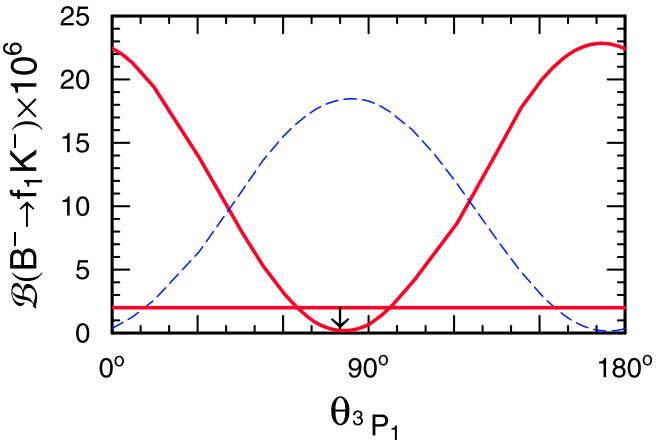

FIG. 1 (color online). Branching ratios of $B^- \to f_1(1285)K^-$ (solid line) and $B^- \to f_1(1420)K^-$ (dashed line) versus the mixing angle $\theta_{^3P_1}$. The physical mixing angle is either 28° or 53°. For simplicity, only the central values are shown here. The horizontal line is the experimental limit on $B^- \to f_1(1285)K^-$.

2.0×10^{-6}. However, we cannot extract the upper bound for the $f_1(1420)K^-$ mode due to the lack of information on $\mathcal{B}(f_1(1420) \to \eta\pi\pi)$ and $\mathcal{B}(f_1(1420) \to K_S K^\pm \pi^\mp)$. In Fig. 1 we plot the branching ratios of $B^- \to f_1(1285)K^-$ and $B^- \to f_1(1420)K^-$ as a function of $\theta_{^3P_1}$. We see that the branching fraction of the former at $\theta_{^3P_1} = 53°$ is barely consistent with the experimental limit when the theoretical errors are taken into account. Note that the mixing angle dependence of the $f_1(1420)K^-$ mode is opposite to that of $f_1(1285)K^-$. At this moment, it is too early to draw any conclusions from the data. Certainly, we have to await more measurements to test our predictions.

B. *CP* asymmetries

Direct *CP* asymmetries for various $B \to AP$ decays are summarized in Tables IX, X, and XI. Because of the large suppression of $\bar{B}^0 \to b_1^- \pi^+$ relative to $\bar{B}^0 \to b_1^+ \pi^-$, direct *CP* violation in the latter should be close to the charge asymmetry $\mathcal{A}_{b_1\pi}$ defined below in Eq. (4.11) which has been measured by *BABAR* to be $-0.05 \pm 0.10 \pm 0.02$ [5]. The default results for direct *CP* violation vanishes in the decays $B^0 \to K_1^+ K^-$ and $B^0 \to K_1^- K^+$ (see Table X) as they proceed only through weak annihilation. The major uncertainty with direct *CP* violation comes from the strong phases which are needed to induce partial rate *CP* asymmetries. For penguin-dominated decays, one of the main sources of strong phases comes from ϕ_A defined in Eq. (3.19) which is originated from soft gluon interactions. It is nonperturbative in nature and hence not calculable.

The experimental determination of direct *CP* asymmetries for $a_1^+ \pi^-$ and $a_1^- \pi^+$ is more complicated as $B^0 \to a_1^\pm \pi^\mp$ is not a *CP* eigenstate. The time-dependent *CP* asymmetries are given by

$$\mathcal{A}(t) \equiv \frac{\Gamma(\bar{B}^0(t) \to a_1^\pm \pi^\mp) - \Gamma(B^0(t) \to a_1^\pm \pi^\mp)}{\Gamma(\bar{B}^0(t) \to a_1^\pm \pi^\mp) + \Gamma(B^0(t) \to a_1^\pm \pi^\mp)} = (S \pm \Delta S)\sin(\Delta m t) - (C \pm \Delta C)\cos(\Delta m t), \tag{4.6}$$

where Δm is the mass difference of the two neutral B eigenstates, S is referred to as mixing-induced *CP* asymmetry and C is the direct *CP* asymmetry, while ΔS and ΔC are *CP*-conserving quantities. Defining

$$A_{+-} \equiv A(B^0 \to a_1^+ \pi^-), \qquad A_{-+} \equiv A(B^0 \to a_1^- \pi^+),$$
$$\bar{A}_{-+} \equiv A(\bar{B}^0 \to a_1^- \pi^+), \qquad \bar{A}_{+-} \equiv A(\bar{B}^0 \to a_1^+ \pi^-), \tag{4.7}$$

and

$$\lambda_{+-} = \frac{q}{p}\frac{\bar{A}_{+-}}{A_{+-}}, \qquad \lambda_{-+} = \frac{q}{p}\frac{\bar{A}_{-+}}{A_{-+}}, \tag{4.8}$$

where $q/p = e^{-2i\beta}$ for $a_1\pi$ modes, we have

TABLE IX. Direct *CP* asymmetries (in %) in the decays $B \to a_1(1260)\pi$, $a_1(1260)K$, $b_1(1235)\pi$ and $b_1(1235)K$. See Table VI for the explanation of theoretical errors. Experiments results are taken from [4,5,10,44].

Mode	Theory	Expt.	Mode	Theory	Expt.
$\bar{B}^0 \to a_1^+ \pi^-$	$-3.6^{+0.1+0.3+20.8}_{-0.1-0.5-20.2}$	$7 \pm 21 \pm 15$ [a]	$\bar{B}^0 \to a_1^+ K^-$	$2.6^{+0.0+0.7+10.1}_{-0.1-0.7-11.0}$	$-16 \pm 12 \pm 1$
$\bar{B}^0 \to a_1^- \pi^+$	$-1.9^{+0.0+0.0+14.6}_{-0.0-0.0-14.3}$	$15 \pm 15 \pm 7$ [a]	$\bar{B}^0 \to a_1^0 \bar{K}^0$	$-7.7^{+0.6+2.1+6.8}_{-0.6-2.2-7.0}$	
$\bar{B}^0 \to a_1^0 \pi^0$	$60.1^{+4.6+6.8+37.6}_{-4.9-8.3-60.7}$		$B^- \to a_1^- \bar{K}^0$	$0.8^{+0.0+0.1+0.6}_{-0.0-0.1-0.0}$	$12 \pm 11 \pm 2$
$B^- \to a_1^- \pi^0$	$0.5^{+0.3+0.6+12.0}_{-0.2-0.3-11.0}$		$B^- \to a_1^0 K^-$	$8.4^{+0.3+1.4+10.3}_{-0.3-1.6-12.0}$	
$B^- \to a_1^0 \pi^-$	$-4.3^{+0.3+1.4+14.1}_{-0.3-2.2-14.5}$				
$\bar{B}^0 \to b_1^+ \pi^-$	$-4.0^{+0.2+0.4+26.2}_{-0.0-0.6-25.5}$		$\bar{B}^0 \to b_1^+ K^-$	$5.5^{+0.2+1.2+47.2}_{-0.3-1.2-30.2}$	$-7 \pm 12 \pm 2$
$\bar{B}^0 \to b_1^- \pi^+$	$66.1^{+1.2+7.4+30.3}_{-1.4-4.8-96.6}$		$\bar{B}^0 \to b_1^0 \bar{K}^0$	$-8.6^{+0.8+3.3+8.3}_{-0.8-4.2-25.4}$	
$\bar{B}^0 \to b_1^0 \pi^0$	$53.4^{+6.4+9.0+5.2}_{-6.3-7.3-4.7}$		$B^- \to b_1^- \bar{K}^0$	$1.4^{+0.1+0.1+5.6}_{-0.1-0.1-0.1}$	
$B^- \to b_1^- \pi^0$	$-36.5^{+4.4+18.4+82.2}_{-4.3-17.7-59.6}$		$B^- \to b_1^0 K^-$	$18.7^{+1.6+7.8+57.7}_{-1.7-6.1-44.9}$	$-46 \pm 20 \pm 2$
$B^- \to b_1^0 \pi^-$	$0.9^{+0.6+2.3+18.0}_{-0.4-2.7-20.5}$	$5 \pm 16 \pm 2$			

[a]Taken from [44].

TABLE X. Direct CP asymmetries (in %) the decays $B \to K_1(1270)\pi$, $K_1(1270)K$, $K_1(1400)\pi$ and $K_1(1400)K$ for two different mixing angles $\theta_{K_1} = -37°$ (top) and $-58°$ (bottom).

Mode	Theory	Mode	Theory
$\bar{B}^0 \to K_1^-(1270)\pi^+$	$38.6^{+2.8+10.0+26.0}_{-3.3-13.0-42.9}$	$\bar{B}^0 \to K_1^+(1400)\pi^+$	$-14.3^{+9.0+1.7+45.3}_{-9.5-1.0-48.8}$
$\bar{B}^0 \to \bar{K}_1^0(1270)\pi^0$	$-32.5^{+1.6+7.4+18.7}_{-1.8-7.6-14.8}$	$\bar{B}^0 \to \bar{K}_1^0(1400)\pi^0$	$1.5^{+0.2+0.9+2.3}_{-1.2-0.8-2.2}$
$B^- \to \bar{K}_1^0(1270)\pi^-$	$-0.8^{+0.3+0.1+3.3}_{-0.3-0.2-4.2}$	$B^- \to \bar{K}_1^0(1400)\pi^-$	$2.2^{+0.4+0.1+1.5}_{-0.3-0.1-1.2}$
$\bar{B}^0 \to K_1^-(1270)\pi^0$	$38.8^{+1.9+7.1+24.5}_{-1.8-9.1-2.5}$	$\bar{B}^0 \to K_1^-(1400)\pi^0$	$-12.9^{+7.3+2.2+40.4}_{-6.5-2.7-9.1}$
$\bar{B}^0 \to K_1^-(1270)K^+$	$0^{+0+0+7.3}_{-0-0-7.3}$	$\bar{B}^0 \to K_1^-(1400)K^+$	$0^{+0+0+13.5}_{-0-0-13.5}$
$\bar{B}^0 \to K_1^+(1270)K^-$	$0^{+0+0+40.9}_{-0-0-40.9}$	$\bar{B}^0 \to K_1^+(1400)K^-$	$0^{+0+0+88.9}_{-0-0-88.9}$
$\bar{B}^0 \to \bar{K}_1^0(1270)K^0$	$-31.0^{+3.5+4.4+10.8}_{-3.1-3.5-11.2}$	$\bar{B}^0 \to \bar{K}_1^0(1400)K^0$	$-7.1^{+0.7+14.9+51.1}_{-0.7-5.1-14.0}$
$\bar{B}^0 \to K_1^0(1270)\bar{K}^0$	$-17.9^{+6.0+0.9+3.9}_{-6.4-0.8-3.0}$	$\bar{B}^0 \to K_1^0(1400)\bar{K}^0$	$-65.5^{+4.0+1.4+12.9}_{-4.0-1.4-18.0}$
$B^- \to K_1^0(1270)K^-$	$17.2^{+5.8+4.2+65.0}_{-5.4-2.9-7.6}$	$B^- \to K_1^0(1420)K^-$	$-45.0^{+7.7+1.5+23.7}_{-7.5-1.0-10.8}$
$B^- \to K_1^-(1270)K^0$	$-40.2^{+6.7+2.1+131.3}_{-8.3-5.0-11.7}$	$B^- \to K_1^-(1420)K^0$	$-17.3^{+22.1+26.4+101.8}_{-22.1-36.2-31.2}$
$\bar{B}^0 \to K_1^-(1270)\pi^+$	$33.6^{+2.6+8.5+31.2}_{-2.3-10.1-50.7}$	$\bar{B}^0 \to K_1^-(1400)\pi^+$	$-39.2^{+8.0+1.5+40.7}_{-2.9-2.9-35.4}$
$\bar{B}^0 \to \bar{K}_1^0(1270)\pi^0$	$-29.6^{+1.4+6.8+19.7}_{-1.4-7.9-23.5}$	$\bar{B}^0 \to \bar{K}_1^0(1400)\pi^0$	$0.1^{+4.3+1.3+6.0}_{-5.0-1.2-5.6}$
$B^- \to \bar{K}_1^0(1270)\pi^-$	$-0.5^{+0.2+0.0+2.7}_{-0.2-0.2-2.2}$	$B^- \to \bar{K}_1^0(1400)\pi^-$	$3.1^{+0.2+0.9+3.0}_{-0.1-0.9-1.7}$
$\bar{B}^0 \to K_1^-(1270)\pi^0$	$32.3^{+0.5+5.1+26.5}_{-0.5-6.7-0.7}$	$\bar{B}^0 \to K_1^-(1400)\pi^0$	$-42.2^{+7.2+5.6+33.9}_{-8.5-8.7-12.1}$
$\bar{B}^0 \to K_1^-(1270)K^+$	$0^{+0+0+27.0}_{-0-0-27.0}$	$\bar{B}^0 \to K_1^-(1400)K^+$	$0^{+0+0+19.7}_{-0-0-19.7}$
$\bar{B}^0 \to K_1^+(1270)K^-$	$0^{+0+0+40.1}_{-0-0-40.1}$	$\bar{B}^0 \to K_1^+(1400)K^-$	$0^{+0+0+48.1}_{-0-0-48.1}$
$\bar{B}^0 \to \bar{K}_1^0(1270)K^0$	$-18.0^{+0.5+1.2+1.3}_{-0.6-0.7-0.1}$	$\bar{B}^0 \to \bar{K}_1^0(1400)K^0$	$-24.3^{+2.2+2.4+10.1}_{-2.0-5.2-56.3}$
$\bar{B}^0 \to K_1^0(1270)\bar{K}^0$	$11.0^{+1.0+2.4+13.0}_{-1.2-2.1-11.0}$	$\bar{B}^0 \to K_1^0(1400)\bar{K}^0$	$-63.0^{+4.3+1.7+19.3}_{-3.0-2.4-23.8}$
$B^- \to K_1^0(1270)K^-$	$9.4^{+3.1+3.5+41.7}_{-3.3-2.5-3.3}$	$B^- \to K_1^0(1420)K^-$	$-59.8^{+2.4+1.2+43.3}_{-2.8-1.4-3.9}$
$B^- \to K_1^-(1270)K^0$	$-39.4^{+6.7+4.3+127.7}_{-6.9-7.8-9.7}$	$B^- \to K_1^-(1420)K^0$	$61.1^{+21.6+23.2+36.3}_{-18.0-41.8-25.5}$

TABLE XI. Direct CP asymmetries (in %) in the decays $B \to f_1\pi$, f_1K, $h_1\pi$ and h_1K with $f_1 = f_1(1285)$, $f_1(1420)$ and $h_1 = h_1(1170)$, $h_1(1380)$. We use two different sets of mixing angles, namely, $\theta_{^3P_1} = 27.9°$ and $\theta_{^1P_1} = 25.2°$ (top), corresponding to $\theta_{K_1} = -37°$, and $\theta_{^3P_1} = 53.2°$ and $\theta_{^1P_1} = -18.1°$ (bottom), corresponding to $\theta_{K_1} = -58°$.

Mode	Theory	Mode	Theory
$B^- \to f_1(1285)\pi^-$	$-7.3^{+0.4+0.5+28.0}_{-0.5-0.6-27.5}$	$B^- \to f_1(1420)\pi^-$	$-4.1^{+0.9+0.6+44.6}_{-1.1-0.7-44.2}$
$\bar{B}^0 \to f_1(1285)\pi^0$	$13.8^{+1.7+3.2+52.6}_{-1.7-3.8-58.7}$	$\bar{B}^0 \to f_1(1420)\pi^0$	$-34.0^{+10.3+8.0+112.2}_{-8.1-3.3-66.4}$
$B^- \to f_1(1285)K^-$	$2.5^{+0.3+0.8+6.7}_{-0.2-0.7-8.0}$	$B^- \to f_1(1420)K^-$	$0.8^{+0.1+0.1+1.6}_{-0.1-0.1-1.7}$
$\bar{B}^0 \to f_1(1285)\bar{K}^0$	$1.9^{+0.1+0.4+2.0}_{-0.1-0.4-2.6}$	$\bar{B}^0 \to f_1(1420)\bar{K}^0$	$1.0^{+0.1+0.2+0.9}_{-0.2-0.2-0.8}$
$B^- \to h_1(1170)\pi^-$	$-11.1^{+1.1+1.8+3.4}_{-1.1-2.3-3.7}$	$B^- \to h_1(1380)\pi^-$	$-18.2^{+2.1+3.6+23.3}_{-2.3-5.4-23.3}$
$\bar{B}^0 \to h_1(1170)\pi^0$	$31.6^{+7.5+6.5+58.8}_{-6.8-7.5-76.7}$	$\bar{B}^0 \to h_1(1380)\pi^0$	$-38.7^{+13.9+13.9+124.1}_{-18.7-9.7-72.4}$
$B^- \to h_1(1170)K^-$	$3.5^{+0.8+0.3+14.1}_{-0.7-0.2-16.5}$	$B^- \to h_1(1380)K^-$	$1.3^{+0.2+0.8+12.8}_{-0.5-0.6-18.2}$
$\bar{B}^0 \to h_1(1170)\bar{K}^0$	$1.7^{+0.2+0.2+2.9}_{-0.1-0.1-2.7}$	$\bar{B}^0 \to h_1(1380)\bar{K}^0$	$1.8^{+0.3+0.4+0.4}_{-0.3-0.5-3.7}$
$B^- \to f_1(1285)\pi^-$	$-7.1^{+0.4+0.5+28.6}_{-0.4-0.6-28.0}$	$B^- \to f_1(1420)\pi^-$	$-3.8^{+0.3+0.4+26.4}_{-0.4-0.4-26.0}$
$\bar{B}^0 \to f_1(1285)\pi^0$	$14.7^{+1.7+3.0+57.0}_{-1.9-3.8-64.0}$	$\bar{B}^0 \to f_1(1420)\pi^0$	$21.0^{+3.2+7.0+40.2}_{-2.7-6.5-45.0}$
$B^- \to f_1(1285)K^-$	$2.5^{+0.3+0.9+3.1}_{-0.3-0.7-1.4}$	$B^- \to f_1(1420)K^-$	$1.3^{+0.3+0.3+3.4}_{-0.2-0.3-3.5}$
$\bar{B}^0 \to f_1(1285)\bar{K}^0$	$2.1^{+0.2+0.6+2.5}_{-0.1-0.5-3.1}$	$\bar{B}^0 \to f_1(1420)\bar{K}^0$	$1.1^{+0.2+0.2+1.1}_{-0.1-0.2-1.2}$
$B^- \to h_1(1170)\pi^-$	$-8.4^{+0.7+1.3+7.2}_{-0.8-1.7-7.9}$	$B^- \to h_1(1380)\pi^-$	$-13.8^{+1.4+2.3+1.4}_{-1.3-2.9-1.4}$
$\bar{B}^0 \to h_1(1170)\pi^0$	$24.9^{+7.2+2.8+46.5}_{-5.6-3.2-52.1}$	$\bar{B}^0 \to h_1(1380)\pi^0$	$56.0^{+3.7+11.2+53.5}_{-4.1-13.6-116.3}$
$B^- \to h_1(1170)K^-$	$5.0^{+2.2+0.8+13.7}_{-1.4-0.9-12.4}$	$B^- \to h_1(1380)K^-$	$-8.1^{+0.4+3.6+4.4}_{-0.2-3.5-4.0}$
$\bar{B}^0 \to h_1(1170)\bar{K}^0$	$0.7^{+0.2+0.2+2.1}_{-0.2-0.2-2.1}$	$\bar{B}^0 \to h_1(1380)\bar{K}^0$	$1.5^{+0.5+0.3+1.6}_{-0.6-0.5-1.5}$

$$C + \Delta C = \frac{1 - |\lambda_{+-}|^2}{1 + |\lambda_{+-}|^2} = \frac{|A_{+-}|^2 - |\bar{A}_{+-}|^2}{|A_{+-}|^2 + |\bar{A}_{+-}|^2},$$
$$C - \Delta C = \frac{1 - |\lambda_{-+}|^2}{1 + |\lambda_{-+}|^2} = \frac{|A_{-+}|^2 - |\bar{A}_{-+}|^2}{|A_{-+}|^2 + |\bar{A}_{-+}|^2}, \quad (4.9)$$

and

$$S + \Delta S \equiv \frac{2\,\mathrm{Im}\lambda_{+-}}{1 + |\lambda_{+-}|^2} = \frac{2\,\mathrm{Im}(e^{-2i\beta}\bar{A}_{+-}A^*_{+-})}{|A_{+-}|^2 + |\bar{A}_{+-}|^2},$$
$$S - \Delta S \equiv \frac{2\,\mathrm{Im}\lambda_{-+}}{1 + |\lambda_{-+}|^2} = \frac{2\,\mathrm{Im}(e^{-2i\beta}\bar{A}_{-+}A^*_{-+})}{|A_{-+}|^2 + |\bar{A}_{-+}|^2}. \quad (4.10)$$

Hence we see that ΔS describes the strong phase difference between the amplitudes contributing to $B^0 \to a_1^\pm \pi^\mp$ and ΔC measures the asymmetry between $\Gamma(B^0 \to a_1^+\pi^-) + \Gamma(\bar{B}^0 \to a_1^-\pi^+)$ and $\Gamma(B^0 \to a_1^-\pi^+) + \Gamma(\bar{B}^0 \to a_1^+\pi^-)$.

Next consider the time- and flavor-integrated charge asymmetry

$$\mathcal{A}_{a_1\pi} \equiv \frac{|A_{+-}|^2 + |\bar{A}_{+-}|^2 - |A_{-+}|^2 - |\bar{A}_{-+}|^2}{|A_{+-}|^2 + |\bar{A}_{+-}|^2 + |A_{-+}|^2 + |\bar{A}_{-+}|^2}. \quad (4.11)$$

Then, following [38] one can transform the experimentally motivated CP parameters $\mathcal{A}_{a_1\pi}$ and $C_{a_1\pi}$ into the physically motivated choices

$$A_{a_1^+\pi^-} \equiv \frac{|\kappa^{-+}|^2 - 1}{|\kappa^{-+}|^2 + 1}, \qquad A_{a_1^-\pi^+} \equiv \frac{|\kappa^{+-}|^2 - 1}{|\kappa^{+-}|^2 + 1}, \quad (4.12)$$

with

$$\kappa^{+-} = \frac{q}{p}\frac{\bar{A}_{-+}}{A_{+-}}, \qquad \kappa^{-+} = \frac{q}{p}\frac{\bar{A}_{+-}}{A_{-+}}. \quad (4.13)$$

Hence,

$$A_{a_1^+\pi^-} = \frac{\Gamma(\bar{B}^0 \to a_1^+\pi^-) - \Gamma(B^0 \to a_1^-\pi^+)}{\Gamma(\bar{B}^0 \to a_1^+\pi^-) + \Gamma(B^0 \to a_1^-\pi^+)} = \frac{\mathcal{A}_{a_1\pi} - C_{a_1\pi} - \mathcal{A}_{a_1\pi}\Delta C_{a_1\pi}}{1 - \Delta C_{a_1\pi} - \mathcal{A}_{a_1\pi}C_{a_1\pi}},$$
$$A_{a_1^-\pi^+} = \frac{\Gamma(\bar{B}^0 \to a_1^-\pi^+) - \Gamma(B^0 \to a_1^+\pi^-)}{\Gamma(\bar{B}^0 \to a_1^-\pi^+) + \Gamma(B^0 \to a_1^+\pi^-)} = -\frac{\mathcal{A}_{a_1\pi} + C_{a_1\pi} + \mathcal{A}_{a_1\pi}\Delta C_{a_1\pi}}{1 + \Delta C_{a_1\pi} + \mathcal{A}_{a_1\pi}C_{a_1\pi}}. \quad (4.14)$$

Note that the quantities $A_{a_1^\pm\pi^\mp}$ here correspond to $A_{a_1^\mp\pi^\pm}$ defined in [38]. Therefore, direct CP asymmetries $A_{a_1^+\pi^-}$ and $A_{a_1^-\pi^+}$ are determined from the above two equations.

Defining the effective phases

$$\alpha^+_{\rm eff} \equiv \tfrac{1}{2}\arg\kappa^{+-} = \tfrac{1}{2}\arg(e^{-2i\beta}\bar{A}_{-+}A^*_{+-}),$$
$$\alpha^-_{\rm eff} \equiv \tfrac{1}{2}\arg\kappa^{-+} = \tfrac{1}{2}\arg(e^{-2i\beta}\bar{A}_{+-}A^*_{-+}), \quad (4.15)$$

which reduce to the unitarity angle α in the absence of penguin contributions, we have

TABLE XII. Various CP parameters for the decays $B^0 \to a_1^\pm\pi^\mp$ (top) and $B^0 \to b_1^\pm\pi^\mp$ (bottom). The parameters S and ΔS are computed for $\beta = 22.1°$ and $\gamma = 68.0°$. Experimental results are taken from [4,5].

Parameter	Theory	Experiment
$\mathcal{A}_{a_1\pi}$	$0.003^{+0.001+0.002+0.043}_{-0.002-0.003-0.045}$	$-0.07 \pm 0.07 \pm 0.02$
C	$0.02^{+0.00+0.00+0.14}_{-0.00-0.00-0.14}$	$-0.10 \pm 0.15 \pm 0.09$
S	$-0.37^{+0.01+0.05+0.09}_{-0.01-0.08-0.16}$	$0.37 \pm 0.21 \pm 0.07$
ΔC	$0.44^{+0.03+0.03+0.03}_{-0.04-0.05-0.04}$	$0.26 \pm 0.15 \pm 0.07$
ΔS	$0.01^{+0.00+0.00+0.02}_{-0.00-0.00-0.02}$	$-0.14 \pm 0.21 \pm 0.06$
$\alpha^+_{\rm eff}$	$(97.2^{+0.3+1.0+4.7}_{-0.3-0.6-2.5})°$	
$\alpha^-_{\rm eff}$	$(107.0^{+0.5+3.6+6.6}_{-0.5-2.3-3.7})°$	
$\alpha_{\rm eff}$	$(102.0^{+0.4+2.3+5.7}_{-0.4-1.5-3.1})°$	$(78.6 \pm 7.3)°$
$\mathcal{A}_{b_1\pi}$	$-0.06^{+0.01+0.01+0.23}_{-0.01-0.01-0.23}$	$-0.05 \pm 0.10 \pm 0.02$
C	$-0.03^{+0.01+0.01+0.06}_{-0.02-0.02-0.01}$	$0.22 \pm 0.23 \pm 0.05$ [a]
S	$0.05^{+0.03+0.02+0.15}_{-0.03-0.02-0.26}$	
ΔC	$-0.96^{+0.03+0.02+0.08}_{-0.03-0.03-0.01}$	$-1.04 \pm 0.23 \pm 0.08$
ΔS	$0.12^{+0.04+0.04+0.08}_{-0.03-0.04-0.09}$	
$\alpha^+_{\rm eff}$	$(107.6^{+0.7+3.5+155.4}_{-0.2-4.9-17.8})°$	
$\alpha^-_{\rm eff}$	$(101.3^{+0.4+2.1+4.9}_{-0.4-1.4-8.6})°$	
$\alpha_{\rm eff}$	$(104.4^{+0.6+2.6+80.4}_{-0.3-2.1-1.6})°$	

[a]Our definition of C in Eq. (4.9) has an opposite sign to that defined in [5] for $B \to b_1\pi$ decays.

$$\alpha_{\rm eff} \equiv \frac{1}{2}(\alpha^+_{\rm eff} + \alpha^-_{\rm eff}) = \frac{1}{4}\left[\arcsin\left(\frac{S + \Delta S}{\sqrt{1 - (C + \Delta C)^2}}\right) + \arcsin\left(\frac{S - \Delta S}{\sqrt{1 - (C - \Delta C)^2}}\right)\right]. \quad (4.16)$$

This is a measurable quantity which is equal to the weak phase α in the limit of vanishing penguin amplitudes.

Parameters of the time-dependent decay rate asymmetries of $B^0 \to a_1^\pm\pi^\mp$ are shown in Table XII. It appears that the calculated mixing-induced parameter S is negative and the effective unitarity angle $\alpha_{\rm eff}$ deviates from experiment by around 2σ. As pointed out by one of us (K.C.Y.), this discrepancy may be resolved by having a larger $\gamma \gtrsim 80°$ (see Fig. 1 of [16]). Further precise measurements are needed to clarify the discrepancy. For $B^0 \to b_1^\pm\pi^\mp$ decays, the predicted ΔC agrees with experiment. The fact that this quantity is very close to -1 indicates that the $\bar{B}^0 \to b_1^-\pi^+$ mode is highly suppressed relative to the $\bar{B}^0 \to b_1^+\pi^-$ one, recalling that ΔC here measures the asymmetry between $\Gamma(B^0 \to b_1^+\pi^-) + \Gamma(\bar{B}^0 \to b_1^-\pi^+)$ and $\Gamma(B^0 \to b_1^-\pi^+) + \Gamma(\bar{B}^0 \to b_1^+\pi^-)$.

C. Comparison with other works

There are several papers studying charmless $B \to AP$ decays: Laporta, Nardulli, and Pham (LNP) [14] (see also

Nardulli and Pham [13]), and Calderón, Muñoz, and Vera (CMV) [15]. Their predictions are shown in Tables VI and VII. Both are based on naive factorization. While form factors are obtained by CMV using the ISGW2 model, LNP use ratios of branching ratios to deduce ratios of form factors. Hence, the relevant form factors are determined by factorization and experimental data. Specifically, LNP found

$$\frac{V_0^{Ba_1}(0)}{A_0^{B\rho}(0)} \approx \frac{V_0^{BK_{1A}}(0)}{A_0^{BK^*}(0)} = h\sin\theta_{K_1} + k\cos\theta_{K_1},$$
$$\frac{V_0^{Bb_1}(0)}{A_0^{B\rho}(0)} \approx \frac{V_0^{BK_{1B}}(0)}{A_0^{BK^*}(0)} = h\cos\theta_{K_1} - k\sin\theta_{K_1}, \tag{4.17}$$

where the kinematic factors h, k are defined in [14]. Therefore, LNP used two different sets of form factors corresponding to different mixing angle values $\theta_{K_1} = 32^\circ$ and 58°.[7] Since LNP only considered factorizable contributions to $B \to AP$ decays, it turns out that in $B \to K_1\pi$ decays, only the $K_1^-(1400)\pi^0$ and $\bar{K}_1^0(1400)\pi^0$ modes depend on the mixing angle θ_{K_1}. The other $K_1\pi$ rates obtained by LNP (see Table VII) are mixing angle independent.

The predicted rates for $a_1\pi$, $b_1\pi$ and b_1K modes by CMV are generally too large compared to the data, presumably due to too big form factors for $B \to a_1(b_1)$ transition predicted by the ISGW2 model. The relation $\mathcal{B}(\bar{B}^0 \to a_1^+\pi^-) > \mathcal{B}(\bar{B}^0 \to a_1^-\pi^+)$ is in conflict with experiment. A noticeable result found by CMV is that $\mathcal{B}(B^- \to K_1^-(1400)K^0)$ and $\mathcal{B}(\bar{B}^0 \to \bar{K}_1^0(1400)K^0)$ are of order 10^{-6}, while in QCDF they are highly suppressed, of order $10^{-7} - 10^{-8}$.

It is clear from Table VI that in the LNP model, the form factors (4.17) derived using $\theta_{K_1} = 32^\circ$ give a better agreement for $a_1\pi$ modes, whereas $\theta_{K_1} = 58^\circ$ is preferred by $b_1\pi$ and b_1K data. This indicates that the data of $a_1(\pi, K)$ and $b_1(\pi, K)$ cannot be simultaneously accounted for by a single mixing angle θ_{K_1} in this model.

Branching ratios of $B \to f_1P$ and $B \to h_1P$ are found to be of order 10^{-5} for $P = \pi^\pm$, η, η', K and $\mathcal{O}(10^{-7})$ for $P = \pi^0$ by CMV. In general, the CMV's predictions are larger than ours by 1 order of magnitude.

V. CONCLUSIONS

In this work we have studied the two-body hadronic decays of B mesons into pseudoscalar and axial-vector mesons within the framework of QCD factorization. The light cone distribution amplitudes for $^3P_1$ and $^1P_1$ axial-vector mesons have been evaluated using the QCD sum rule method. Owing to the G-parity, the chiral-even two-parton light cone distribution amplitudes of the $^3P_1$ ($^1P_1$) mesons are symmetric (antisymmetric) under the exchange of quark and antiquark momentum fractions in the SU(3) limit. For chiral-odd light cone distribution amplitudes, it is other way around. Our main conclusions are as follows:

(i) Using the Gell-Mann-Okubo mass formula and the $K_1(1270)$ and $K_1(1400)$ mixing angle $\theta_{K_1} = -37^\circ(-58^\circ)$, the mixing angles for $^3P_1$ and $^1P_1$ states are found to be $\theta_{^3P_1} \sim 28^\circ(53^\circ)$ for the $f_1(1420)$ and $f_1(1285)$ and $\theta_{^1P_1} \sim 25^\circ(-18^\circ)$ for $h_1(1170)$ and the $h_1(1380)$, respectively.

(ii) The predicted rates for $a_1^\pm(1260)\pi^\mp$, $b_1^\pm(1235)\pi^\mp$, $b_1^0(1235)\pi^-$, $a_1^+K^-$ and $b_1^+K^-$ modes are in good agreement with the data. However, the expected ratios $\mathcal{B}(B^- \to a_1^0\pi^-)/\mathcal{B}(\bar{B}^0 \to a_1^+\pi^-) \lesssim 1$, $\mathcal{B}(B^- \to a_1^-\pi^0)/\mathcal{B}(\bar{B}^0 \to a_1^-\pi^+) \sim \frac{1}{2}$ and $\mathcal{B}(B^- \to b_1^0K^-)/\mathcal{B}(\bar{B}^0 \to b_1^+K^-) \sim \frac{1}{2}$ are not borne out by experiment. This should be clarified by the improved measurements of these decays in the future.

(iii) One of the salient features of the $^1P_1$ axial-vector meson is that its axial-vector decay constant is small, vanishing in the SU(3) limit. This feature is confirmed by the observation that $\Gamma(\bar{B}^0 \to b_1^-\pi^+) \ll \Gamma(\bar{B}^0 \to b_1^+\pi^-)$. By contrast, it is expected that $\Gamma(\bar{B}^0 \to a_1^-\pi^+) \gg \Gamma(\bar{B}^0 \to a_1^+\pi^-)$ due to the fact that $f_{a_1} \gg f_\pi$.

(iv) While $B \to a_1\pi$ decays have similar rates as that of $B \to \rho\pi$, the penguin-dominated decays $B \to a_1K$ resemble much more to the πK modes than ρK ones. However, the naively expected ratio $\mathcal{B}(B^- \to a_1^-\bar{K}^0)/\mathcal{B}(\bar{B}^0 \to a_1^+K^-) \approx \mathcal{B}(B^- \to \pi^-\bar{K}^0)/\mathcal{B}(\bar{B}^0 \to \pi^+K^-) \approx 1.2$ is not consistent with the current experimental value of 2.14 ± 0.63.

(v) Since the $\bar{B} \to b_1K$ decays receive sizable annihilation contributions, their rates are sensitive to the interference between penguin and annihilation terms. The measurement of $\mathcal{B}(\bar{B}^0 \to b_1^+K^-)$ implies a destructive interference which in turn indicates that the form factors for $B \to b_1$ and $B \to a_1$ transitions must be of opposite signs.

(vi) The central values of the branching ratios for the penguin-dominated modes $K_1^-(1270)\pi^+$ and $K_1^-(1400)\pi^+$ predicted by QCD factorization are too small compared to experiment. Just as the case of $B \to K^*\pi$ decays, sizable power corrections such as weak annihilation are needed to account for the observed $K_1\pi$ rates. The current measurement of $\bar{B}^0 \to K_1^-(1400)\pi^+$ seems to favor a $K_{1A} - K_{1B}$ mixing angle of -37° over -58°.

(vii) The decays $B \to K_1\bar{K}$ with $K_1 = K_1(1270)$ and $K_1(1400)$ are in general quite suppressed, of order $10^{-7} \sim 10^{-8}$, except for $\bar{B}^0 \to \bar{K}_1^0(1270)K^0$ which

[7] Since the $B \to K_{1A}$ and $B \to K_{1B}$ form factors obtained in the ISGW2 model are opposite in sign, the preferred mixing angle θ_{K_1} should be negative, as discussed in Sec. II A.

can have a branching ratio of order 2.3×10^{-6}. The decay modes $K_1^- K^+$ and $K_1^+ K^-$ are of particular interest as they are the only AP modes that proceed only through weak annihilation.

(viii) Time-dependent CP asymmetries in the decays $B^0 \to a_1^\pm \pi^\mp$ and $b_1^\pm \pi^\mp$ are studied. For the former, the mixing-induced parameter S is found to be negative and the effective unitarity angle $\alpha_{\rm eff}$ deviates from experiment by around 2σ. The discrepancy between theory and experiment may be resolved by having a larger $\gamma \gtrsim 80^\circ$. Further precise measurements are needed to clarify the discrepancy.

(ix) Branching ratios for the decays $B \to f_1\pi$, $f_1 K$, $h_1\pi$ and $h_1 K$ with $f_1 = f_1(1285)$, $f_1(1420)$ and $h_1 = h_1(1170)$, $h_1(1380)$ are generally of order 10^{-6} except for the color-suppressed $f_1\pi^0$ and $h_1\pi^0$ modes which are suppressed by one to 2 orders of magnitude. Measurements of the ratios $\mathcal{B}(B^- \to h_1(1380)\pi^-)/\mathcal{B}(B^- \to h_1(1170)\pi^-)$ and $\mathcal{B}(\bar{B} \to f_1(1420)\bar{K})/\mathcal{B}(\bar{B} \to f_1(1285)\bar{K})$ will help determine the mixing angles $\theta_{^1P_1}$ and $\theta_{^3P_1}$, respectively.

ACKNOWLEDGMENTS

We are grateful to Jim Smith for reading the manuscript and for valuable comments. This research was supported in part by the National Science Council of R.O.C. under Grant Nos. NSC96-2112-M-001-003 and NSC96-2112-M-033-004-MY3.

APPENDIX: DECAY AMPLITUDES

For simplicity, here we do not explicitly show the arguments, M_1 and M_2, of α_i^p and β_i^p coefficients. The order of the arguments of the $\alpha_i^p(M_1M_2)$ and $\beta_i^p(M_1M_2)$ is consistent with the order of the arguments of the $X^{(\bar{B}M_1,M_2)}$, where

$$\beta_i^p(M_1M_2) = \frac{-if_B f_{M_1} f_{M_2}}{X^{(\bar{B}M_1,M_2)}} b_i^p. \tag{A1}$$

Within the framework of QCD factorization [37], the $B \to AP$ decay amplitudes read

$$\begin{aligned}
\sqrt{2}\mathcal{A}_{B^-\to a_1^0\pi^-} &= \frac{G_F}{\sqrt{2}} \sum_{p=u,c} \lambda_p^{(d)} \Big\{ \Big[\delta_{pu}(\alpha_2 - \beta_2) - \alpha_4^p + \frac{3}{2}\alpha_{3,\rm EW}^p + \frac{1}{2}\alpha_{4,\rm EW}^p - \beta_3^p - \beta_{3,\rm EW}^p \Big] X^{(\bar{B}\pi,a_1)} \\
&\quad + [\delta_{pu}(\alpha_1 + \beta_2) + \alpha_4^p + \alpha_{4,\rm EW}^p + \beta_3^p + \beta_{3,\rm EW}^p] X^{(\bar{B}a_1,\pi)} \Big\}, \\
\sqrt{2}\mathcal{A}_{B^-\to a_1^-\pi^0} &= \frac{G_F}{\sqrt{2}} \sum_{p=u,c} \lambda_p^{(d)} \Big\{ \Big[\delta_{pu}(\alpha_2 - \beta_2) - \alpha_4^p + \frac{3}{2}\alpha_{3,\rm EW}^p + \frac{1}{2}\alpha_{4,\rm EW}^p - \beta_3^p - \beta_{3,\rm EW}^p \Big] X^{(\bar{B}a_1,\pi)} \\
&\quad + [\delta_{pu}(\alpha_1 + \beta_2) + \alpha_4^p + \alpha_{4,\rm EW}^p + \beta_3^p + \beta_{3,\rm EW}^p] X^{(\bar{B}\pi,a_1)} \Big\}, \\
\mathcal{A}_{\bar{B}^0\to a_1^-\pi^+} &= \frac{G_F}{\sqrt{2}} \sum_{p=u,c} \lambda_p^{(d)} \Big\{ \Big[\delta_{pu}\alpha_1 + \alpha_4^p + \alpha_{4,\rm EW}^p + \beta_3^p + \beta_4^p - \frac{1}{2}\beta_{3,\rm EW}^p - \frac{1}{2}\beta_{4,\rm EW}^p \Big] X^{(\bar{B}\pi,a_1)} \\
&\quad + [\delta_{pu}\beta_1 + \beta_4^p + \beta_{4,\rm EW}^p] X^{(\bar{B}a_1,\pi)} \Big\}, \\
\mathcal{A}_{\bar{B}^0\to a_1^+\pi^-} &= \frac{G_F}{\sqrt{2}} \sum_{p=u,c} \lambda_p^{(d)} \Big\{ \Big[\delta_{pu}\alpha_1 + \alpha_4^p + \alpha_{4,\rm EW}^p + \beta_3^p + \beta_4^p - \frac{1}{2}\beta_{3,\rm EW}^p - \frac{1}{2}\beta_{4,\rm EW}^p \Big] X^{(\bar{B}a_1,\pi)} \\
&\quad + [\delta_{pu}\beta_1 + \beta_4^p + \beta_{4,\rm EW}^p] X^{(\bar{B}\pi,a_1)} \Big\}, \\
-2\mathcal{A}_{\bar{B}^0\to \pi^0 a_1^0} &= \frac{G_F}{\sqrt{2}} \sum_{p=u,c} \lambda_p^{(d)} \Big\{ \Big[\delta_{pu}(\alpha_2 - \beta_1) - \alpha_4^p + \frac{3}{2}\alpha_{3,\rm EW}^p + \frac{1}{2}\alpha_{4,\rm EW}^p - \beta_3^p - 2\beta_4^p + \frac{1}{2}\beta_{3,\rm EW}^p - \frac{1}{2}\beta_{4,\rm EW}^p \Big] X^{(\bar{B}\pi,a_1)} \\
&\quad + \Big[\delta_{pu}(\alpha_2 - \beta_1) - \alpha_4^p + \frac{3}{2}\alpha_{3,\rm EW}^p + \frac{1}{2}\alpha_{4,\rm EW}^p - \beta_3^p - 2\beta_4^p + \frac{1}{2}\beta_{3,\rm EW}^p - \frac{1}{2}\beta_{4,\rm EW}^p \Big] X^{(\bar{B}a_1,\pi)} \Big\},
\end{aligned} \tag{A2}$$

for $\bar{B} \to a_1\pi$,

$$
\begin{aligned}
\mathcal{A}_{B^-\to a_1^-\bar{K}^0} &= \frac{G_F}{\sqrt{2}}\sum_{p=u,c}\lambda_p^{(s)}\Big[\delta_{pu}\beta_2+\alpha_4^p-\frac{1}{2}\alpha_{4,\mathrm{EW}}^p+\beta_3^p+\beta_{3,\mathrm{EW}}^p\Big]X^{(\bar{B}a_1,\bar{K})},\\
\sqrt{2}\mathcal{A}_{B^-\to a_1^0K^-} &= \frac{G_F}{\sqrt{2}}\sum_{p=u,c}\lambda_p^{(s)}\Big\{\Big[\delta_{pu}(\alpha_1+\beta_2)+\alpha_4^p+\alpha_{4,\mathrm{EW}}^p+\beta_3^p+\beta_{3,\mathrm{EW}}^p\Big]X^{(\bar{B}a_1,\bar{K})}+\Big[\delta_{pu}\alpha_2+\frac{3}{2}\alpha_{3,\mathrm{EW}}^p\Big]X^{(\bar{B}\bar{K},a_1)}\Big\},\\
\mathcal{A}_{\bar{B}^0\to a_1^+K^-} &= \frac{G_F}{\sqrt{2}}\sum_{p=u,c}\lambda_p^{(s)}\Big[\delta_{pu}\alpha_1+\alpha_4^p+\alpha_{4,\mathrm{EW}}^p+\beta_3^p-\frac{1}{2}\beta_{3,\mathrm{EW}}^p\Big]X^{(\bar{B}a_1,\bar{K})},\\
\sqrt{2}\mathcal{A}_{\bar{B}^0\to a_1^0\bar{K}^0} &= \frac{G_F}{\sqrt{2}}\sum_{p=u,c}\lambda_p^{(s)}\Big\{\Big[-\alpha_4^p+\frac{1}{2}\alpha_{4,\mathrm{EW}}^p-\beta_3^p+\frac{1}{2}\beta_{3,\mathrm{EW}}^p\Big]X^{(\bar{B}a_1,\bar{K})}+\Big[\delta_{pu}\alpha_2+\frac{3}{2}\alpha_{3,\mathrm{EW}}^p\Big]X^{(\bar{B}\bar{K},a_1)}\Big\},
\end{aligned}
\tag{A3}
$$

for $\bar{B}\to a_1\bar{K}$,

$$
\begin{aligned}
\sqrt{2}\mathcal{A}_{B^-\to f_1^0\pi^-} &= \frac{G_F}{\sqrt{2}}\sum_{p=u,c}\lambda_p^{(d)}\Big\{\Big[\delta_{pu}(\alpha_2+\beta_2)+2\alpha_3^p+\alpha_4^p+\frac{1}{2}\alpha_{3,\mathrm{EW}}^p-\frac{1}{2}\alpha_{4,\mathrm{EW}}^p+\beta_3^p+\beta_{3,\mathrm{EW}}^p\Big]X^{(\bar{B}\pi,f_1^q)}\\
&\quad+\sqrt{2}\Big[\alpha_3^p-\frac{1}{2}\alpha_{3,\mathrm{EW}}^p\Big]X^{(\bar{B}\pi,f_1^s)}+[\delta_{pu}(\alpha_1+\beta_2)+\alpha_4^p+\alpha_{4,\mathrm{EW}}^p+\beta_3^p+\beta_{3,\mathrm{EW}}^p]X^{(\bar{B}f_1^q,\pi)}\Big\},\\
-2\mathcal{A}_{\bar{B}^0\to f_1^0\pi^0} &= \frac{G_F}{\sqrt{2}}\sum_{p=u,c}\lambda_p^{(d)}\Big\{\Big[\delta_{pu}(\alpha_2-\beta_1)+2\alpha_3^p+\alpha_4^p+\frac{1}{2}\alpha_{3,\mathrm{EW}}^p-\frac{1}{2}\alpha_{4,\mathrm{EW}}^p+\beta_3^p-\frac{1}{2}\beta_{3,\mathrm{EW}}^p-\frac{3}{2}\beta_{4,\mathrm{EW}}^p\Big]X^{(\bar{B}\pi,f_1^q)}\\
&\quad+\sqrt{2}\Big[\alpha_3^p-\frac{1}{2}\alpha_{3,\mathrm{EW}}^p\Big]X^{(\bar{B}\pi,f_1^s)}\\
&\quad+\Big[\delta_{pu}(-\alpha_2-\beta_1)+\alpha_4^p-\frac{3}{2}\alpha_{3,\mathrm{EW}}^p-\frac{1}{2}\alpha_{4,\mathrm{EW}}^p+\beta_3^p-\frac{1}{2}\beta_{3,\mathrm{EW}}^p-\frac{3}{2}\beta_{4,\mathrm{EW}}^p\Big]X^{(\bar{B}f_1^q,\pi)}\Big\},\\
\sqrt{2}\mathcal{A}_{B^-\to f_1^0K^-} &= \frac{G_F}{\sqrt{2}}\sum_{p=u,c}\lambda_p^{(s)}\Big\{\Big[\delta_{pu}\alpha_2+2\alpha_3^p+\frac{1}{2}\alpha_{3,\mathrm{EW}}^p\Big]X^{(\bar{B}K,f_1^q)}\\
&\quad+\sqrt{2}\Big[\delta_{pu}\beta_2+\alpha_3^p+\alpha_4^p-\frac{1}{2}\alpha_{3,\mathrm{EW}}^p-\frac{1}{2}\alpha_{4,\mathrm{EW}}^p+\beta_3^p+\beta_{3,\mathrm{EW}}^p\Big]X^{(\bar{B}K,f_1^s)}\\
&\quad+[\delta_{pu}(\alpha_1+\beta_2)+\alpha_4^p+\alpha_{4,\mathrm{EW}}^p+\beta_3^p+\beta_{3,\mathrm{EW}}^p]X^{(\bar{B}f_1^q,K)}\},\\
\sqrt{2}\mathcal{A}_{\bar{B}^0\to f_1^0\bar{K}^0} &= \frac{G_F}{\sqrt{2}}\sum_{p=u,c}\lambda_p^{(s)}\Big\{\Big[\delta_{pu}\alpha_2+2\alpha_3^p+\frac{1}{2}\alpha_{3,\mathrm{EW}}^p\Big]X^{(\bar{B}K,f_1^q)}\\
&\quad+\sqrt{2}\Big[\alpha_3^p+\alpha_4^p-\frac{1}{2}\alpha_{3,\mathrm{EW}}^p-\frac{1}{2}\alpha_{4,\mathrm{EW}}^p+\beta_3^p-\frac{1}{2}\beta_{3,\mathrm{EW}}^p\Big]X^{(\bar{B}K,f_1^s)}\\
&\quad+\Big[\alpha_4^p-\frac{1}{2}\alpha_{4,\mathrm{EW}}^p+\beta_3^p-\frac{1}{2}\beta_{3,\mathrm{EW}}^p\Big]X^{(\bar{B}f_1^q,K)}\Big\},
\end{aligned}
\tag{A4}
$$

for $\bar{B}\to f_1^0\pi$ and $\bar{B}\to f_1^0\bar{K}$,

$$
\begin{aligned}
\mathcal{A}_{B^-\to\bar{K}_1^0\pi^-} &= \frac{G_F}{\sqrt{2}}\sum_{p=u,c}\lambda_p^{(s)}\Big[\delta_{pu}\beta_2+\alpha_4^p-\frac{1}{2}\alpha_{4,\mathrm{EW}}^p+\beta_3^p+\beta_{3,\mathrm{EW}}^p\Big]X^{(\bar{B}\pi,\bar{K}_1)},\\
\sqrt{2}\mathcal{A}_{B^-\to K_1^-\pi^0} &= \frac{G_F}{\sqrt{2}}\sum_{p=u,c}\lambda_p^{(s)}\Big\{[\delta_{pu}(\alpha_1+\beta_2)+\alpha_4^p+\alpha_{4,\mathrm{EW}}^p+\beta_3^p+\beta_{3,\mathrm{EW}}^p]X^{(\bar{B}\pi,\bar{K}_1)}+\Big[\delta_{pu}\alpha_2+\frac{3}{2}\alpha_{3,\mathrm{EW}}^p\Big]X^{(\bar{B}\bar{K}_1,\pi)}\Big\},\\
\mathcal{A}_{\bar{B}^0\to K_1^-\pi^+} &= \frac{G_F}{\sqrt{2}}\sum_{p=u,c}\lambda_p^{(s)}[\delta_{pu}\alpha_1+\alpha_4^p+\alpha_{4,\mathrm{EW}}^p+\beta_3^p-\frac{1}{2}\beta_{3,\mathrm{EW}}^p]X^{(\bar{B}\pi,\bar{K}_1)},\\
\sqrt{2}\mathcal{A}_{\bar{B}^0\to\bar{K}_1^0\pi^0} &= \frac{G_F}{\sqrt{2}}\sum_{p=u,c}\lambda_p^{(s)}\Big\{\Big[-\alpha_4^p+\frac{1}{2}\alpha_{4,\mathrm{EW}}^p-\beta_3^p+\frac{1}{2}\beta_{3,\mathrm{EW}}^p\Big]X^{(\bar{B}\pi,\bar{K}_1)}+\Big[\delta_{pu}\alpha_2+\frac{3}{2}\alpha_{3,\mathrm{EW}}^p\Big]X^{(\bar{B}\bar{K}_1,\pi)}\Big\},
\end{aligned}
\tag{A5}
$$

for $\bar{B}\to\bar{K}_1\pi$, and

$$
\begin{aligned}
\mathcal{A}_{B^-\to K_1^- K^0} &= \frac{G_F}{\sqrt{2}}\sum_{p=u,c}\lambda_p^{(d)}\Big[\delta_{pu}\beta_2+\alpha_4^p-\frac{1}{2}\alpha_{4,\rm EW}^p+\beta_3^p+\beta_{3,\rm EW}^p\Big]X^{(\bar B\bar K_1,K)},\\
\mathcal{A}_{B^-\to K_1^0 K^-} &= \frac{G_F}{\sqrt{2}}\sum_{p=u,c}\lambda_p^{(d)}\Big[\delta_{pu}\beta_2+\alpha_4^p-\frac{1}{2}\alpha_{4,\rm EW}^p+\beta_3^p+\beta_{3,\rm EW}^p\Big]X^{(\bar B\bar K,K_1)},\\
\mathcal{A}_{\bar B^0\to K_1^- K^+} &= \frac{G_F}{\sqrt{2}}\sum_{p=u,c}\lambda_p^{(d)}\Big\{\Big[\delta_{pu}\beta_1+\beta_4^p+\beta_{4,\rm EW}^p\Big]X^{(\bar BK_1,K)}+f_Bf_{K_1}f_K\Big[b_4^p-\frac{1}{2}b_{4,\rm EW}^p\Big]_{KK_1}\Big\},\\
\mathcal{A}_{\bar B^0\to K_1^+ K^-} &= \frac{G_F}{\sqrt{2}}\sum_{p=u,c}\lambda_p^{(d)}\Big\{[\delta_{pu}\beta_1+\beta_4^p+\beta_{4,\rm EW}^p]X^{(\bar BK,K_1)}+f_Bf_{K_1}f_K\Big[b_4^p-\frac{1}{2}b_{4,\rm EW}^p\Big]_{K_1K}\Big\},\\
\mathcal{A}_{\bar B^0\to \bar K_1^0 K^0} &= \frac{G_F}{\sqrt{2}}\sum_{p=u,c}\lambda_p^{(d)}\Big\{\Big[\alpha_4^p-\frac{1}{2}\alpha_{4,\rm EW}^p+\beta_3^p+\beta_4^p-\frac{1}{2}\beta_{3,\rm EW}^p-\frac{1}{2}\beta_{4,\rm EW}^p\Big]X^{(\bar B\bar K_1,K)}+f_Bf_{K_1}f_K\Big[b_4^p-\frac{1}{2}b_{4,\rm EW}^p\Big]_{K\bar K_1}\Big\},\\
\mathcal{A}_{\bar B^0\to K_1^0 \bar K^0} &= \frac{G_F}{\sqrt{2}}\sum_{p=u,c}\lambda_p^{(d)}\Big\{\Big[\alpha_4^p-\frac{1}{2}\alpha_{4,\rm EW}^p+\beta_3^p+\beta_4^p-\frac{1}{2}\beta_{3,\rm EW}^p-\frac{1}{2}\beta_{4,\rm EW}^p\Big]X^{(\bar B\bar K,K_1)}+f_Bf_{K_1}f_K\Big[b_4^p-\frac{1}{2}b_{4,\rm EW}^p\Big]_{K_1\bar K}\Big\},
\end{aligned}
\tag{A6}
$$

for $\bar B\to \bar K_1 K$ and $\bar B\to K_1\bar K$, where $\lambda_p^{(d)}\equiv V_{pb}V_{pd}^*$, $\lambda_p^{(s)}\equiv V_{pb}V_{ps}^*$, and the factorizable amplitudes $X^{(\bar BA,P)}$ and $X^{(\bar BP,A)}$ are defined in Eq. (2.48). The decay amplitudes for $\bar B\to b_1\pi$ and $b_1\bar K$ are obtained from $\bar B\to a_1\pi$ and $a_1\bar K$ respectively by replacing $a_1\to b_1$. Likewise, the expressions for $\bar B\to h_1\pi$, $h_1\bar K$ decay amplitudes are obtained by setting $(f_1\pi\to h_1\pi)$ and $(f_1\bar K\to h_1\bar K)$.

The coefficients of the flavor operators α_i^p read

$$
\begin{aligned}
&\alpha_1(M_1,M_2)=a_1(M_1,M_2), \qquad \alpha_2(M_1M_2)=a_2(M_1M_2),\\
&\alpha_3^p(M_1M_2)=a_3^p(M_1M_2)-a_5^p(M_1M_2), \qquad \alpha_{3,\rm EW}^p(M_1M_2)=a_9^p(M_1M_2)-a_7^p(M_1M_2),\\
&\alpha_4^p(M_1M_2)=\begin{cases}a_4^p(M_1M_2)+r_\chi^P a_6^p(M_1M_2); & \text{for } M_1M_2=AP,\\ a_4^p(M_1M_2)-r_\chi^A a_6^p(M_1M_2); & \text{for } M_1M_2=PA,\end{cases}\\
&\alpha_{4,\rm EW}^p(M_1M_2)=\begin{cases}a_{10}^p(M_1M_2)+r_\chi^P a_8^p(M_1M_2); & \text{for } M_1M_2=AP,\\ a_{10}^p(M_1M_2)-r_\chi^A a_8^p(M_1M_2); & \text{for } M_1M_2=PA,\end{cases}
\end{aligned}
\tag{A7}
$$

where r_χ^P and r_χ^A are defined before in Eq. (3.12).

[1] Y. M. Yao *et al.* (Particle Data Group), J. Phys. G **33**, 1 (2006).
[2] B. Aubert *et al.* (*BABAR* Collaboration), Phys. Rev. Lett. **97**, 051802 (2006).
[3] K. Abe *et al.* (Belle Collaboration), arXiv:0706.3279.
[4] B. Aubert *et al.* (*BABAR* Collaboration), Phys. Rev. Lett. **98**, 181803 (2007).
[5] B. Aubert *et al.* (*BABAR* Collaboration), arXiv:0707.4561.
[6] B. Aubert *et al.* (*BABAR* Collaboration), arXiv:0708.0050.
[7] B. Aubert *et al.* (*BABAR* Collaboration), arXiv:0709.4165.
[8] F. Blanc, Moriond QCD, La Thuile, Italy, March 17–24, 2007 (2007).
[9] J. P. Burke, International Europhysics Conference on High Energy Physics, Manchester, England, July 19–25, 2007 (2007).
[10] D. Brown, XXIII International Symposium on Lepton and Photon Interactions at High Energy, August 13–18, 2007, Daegu, Korea (2007).
[11] K. C. Yang, Phys. Rev. D **72**, 034009 (2005); **72**, 059901(E) (2005).
[12] C. H. Chen, C. Q. Geng, Y. K. Hsiao, and Z. T. Wei, Phys. Rev. D **72**, 054011 (2005).
[13] G. Nardulli and T. N. Pham, Phys. Lett. B **623**, 65 (2005).
[14] V. Laporta, G. Nardulli, and T. N. Pham, Phys. Rev. D **74**, 054035 (2006).
[15] G. Calderón, J. H. Muñoz, and C. E. Vera, Phys. Rev. D **76**, 094019 (2007).
[16] K. C. Yang, Phys. Rev. D **76**, 094002 (2007).
[17] K. C. Yang, J. High Energy Phys. 10 (2005) 108.
[18] K. C. Yang, Nucl. Phys. **B776**, 187 (2007).
[19] H. J. Lipkin, Phys. Lett. **72B**, 249 (1977).
[20] M. Suzuki, Phys. Rev. D **47**, 1252 (1993).
[21] L. Burakovsky and T. Goldman, Phys. Rev. D **56**, R1368 (1997).
[22] H. Y. Cheng, Phys. Rev. D **67**, 094007 (2003).
[23] H. Y. Cheng and C. K. Chua, Phys. Rev. D **69**, 094007 (2004).
[24] H. Y. Cheng, C. K. Chua, and C. W. Hwang, Phys. Rev. D **69**, 074025 (2004).

[25] H. Yang *et al.* (Belle Collaboration), Phys. Rev. Lett. **94**, 111802 (2005).
[26] F. E. Close, *An Introduction to Quarks and Partons* (Academic Press Inc. Ltd., London, 1979).
[27] F. E. Close and A. Kirk, Z. Phys. C **76**, 469 (1997).
[28] R. Barate *et al.* (ALEPH Collaboration), Eur. Phys. J. C **11**, 599 (1999).
[29] K. C. Yang (unpublished).
[30] A. Deandrea, R. Gatto, G. Nardulli, and A. D. Polosa, Phys. Rev. D **59**, 074012 (1999).
[31] D. Scora and N. Isgur, Phys. Rev. D **52**, 2783 (1995).
[32] T. M. Aliev and M. Savci, Phys. Lett. B **456**, 256 (1999).
[33] N. Isgur, D. Scora, B. Grinstein, and M. B. Wise, Phys. Rev. D **39**, 799 (1989).
[34] H. Y. Cheng, C. K. Chua, and K. C. Yang, Phys. Rev. D **73**, 014017 (2006).
[35] M. Diehl and G. Hiller, J. High Energy Phys. 06 (2001) 067.
[36] P. Ball, V. M. Braun, and A. Lenz, J. High Energy Phys. 05 (2006) 004.
[37] M. Beneke, G. Buchalla, M. Neubert, and C. T. Sachrajda, Phys. Rev. Lett. **83**, 1914 (1999); Nucl. Phys. **B591**, 313 (2000); **B606**, 245 (2001).
[38] J. Charles *et al.* (CKMfitter Group), Eur. Phys. J. C **41**, 1 (2005) http://ckmfitter.in2p3.fr; M. Bona *et al.* (UTfit Collaboration), J. High Energy Phys. 07 (2005) 028 http://utfit.roma1.infn.it.
[39] M. Beneke and M. Neubert, Nucl. Phys. **B675**, 333 (2003).
[40] H. Y. Cheng, C. K. Chua, and K. C. Yang, arXiv:0705.3079.
[41] C. W. Bauer, D. Pirjol, I. Z. Rothstein, and I. W. Stewart, Phys. Rev. D **70**, 054015 (2004).
[42] H. Y. Cheng, C. K. Chua, and A. Soni, Phys. Rev. D **71**, 014030 (2005).
[43] M. Beneke, J. Rohrer, and D. S. Yang, Nucl. Phys. **B774**, 64 (2007).
[44] E. Barberio *et al.* (Heavy Flavor Averaging Group), arXiv:0704.3575 http://www.slac.stanford.edu/xorg/hfag.